Published in final edited form as:
*Mol Microbiol*. 2010 January ; 75(2): 376–393. doi:10.1111/j.1365-2958.2009.06973.x.

# C-ring requirement in flagellar type III secretion is bypassed by FlhDC upregulation

**Marc Erhardt**[§] and **Kelly T. Hughes**
Department of Biology, University of Utah, Salt Lake City, UT 84112, USA

## Abstract

The cytoplasmic C-ring of the flagellum consists of FliG, FliM and FliN and acts as an affinity cup to localize secretion substrates for protein translocation via the flagellar-specific type III secretion system. Random T-POP transposon mutagenesis was employed to screen for insertion mutants that allowed flagellar type III secretion in the absence of the C-ring using the flagellar type III secretion system-specific hook-β-lactamase reporter (Lee & Hughes, 2006). Any condition resulting in at least a 2-fold increase in *flhDC* expression was sufficient to overcome the requirement for the C-ring and the ATPase complex FliHIJ in flagellar type III secretion. Insertions in known and unknown flagellar regulatory loci were isolated as well as chromosomal duplications of the *flhDC* region. The 2-fold increased *flhDC* mRNA level coincided in a 2-fold increase in the number of hook-basal-bodies per cell as analyzed by fluorescent microscopy. These results indicate that the C-ring functions as a non-essential affinity cup-like structure during flagellar type III secretion to enhance the specificity and efficiency of the secretion process.

### Keywords

*flhDC* regulation; flagellar type III secretion; C-ring affinity cup; transposon mutagenesis

## Introduction

Many bacteria propel themselves in their environments by rotation of one or more propeller-like appendages called flagella (Berg & Anderson, 1973). The flagellum consists of mainly three structural parts: I) a basal body that spans the inner and outer membranes and is composed of a ion-powered (proton or sodium) rotary-motor, which incorporates a specific type III protein-secretion system, II) an external, flexible hook that acts as a universal joint between the rigid drive-shaft (rod) of the basal motor and III) the rigid, external filament (Berg, 2003, Chevance & Hughes, 2008, Macnab, 2003) (Figure 1A).

The flagellar-specific type III secretion (T3S) apparatus is believed to assemble at the base of the flagellar basal body within the MS-ring (consisting of FliF) in the inner membrane. The core T3S proteins include six integral membrane proteins (FlhA, FlhB, FliO, FliP, FliQ, FliR) and three cytoplasmic proteins (FliH, FliI, FliJ) (Minamino & Macnab, 1999). Recently it was discovered that translocation of substrates across the inner membrane was dependent on the proton motive force (PMF) (Paul *et al.*, 2008, Minamino & Namba, 2008), and is presumably coupled to ATP-dependent substrate release and unfolding (Akeda & Galan, 2005). The ATPase complex $FliH_2IJ$ seems to function in cargo delivery to the C-ring and unfolding of the polypeptide prior to secretion. The FliH dimer has been shown to

[§]Corresponding author Marc Erhardt; Mailing address: Department of Biology, University of Utah, 257 South 1400 East, Salt Lake City, UT, 84112; Tel: +801-585-6950; Fax: +801-585-9735; marc.erhardt@utah.edu.

interact with the C-ring protein FliN (Gonzalez-Pedrajo *et al.*, 2006), thereby presumably targeting substrates to the secretion system.

Beneath the MS-ring in the inner membrane, the cytoplasmic C-ring forms, which consists of FliG, FliM and FliN and is also referred to as the switch complex as this structure forms the rotor of the flagellar motor and controls the clockwise/counterclockwise rotation of the flagellum. The C-ring serves dual roles as the rotor of the flagellar motor and cup-like structure that possibly facilitates docking and secretion of flagellar substrates (Gonzalez-Pedrajo et al., 2006). Flagellar assembly is blocked at an early stage in strains deleted for *fliG*, *fliM*, or *fliN* (Kubori *et al.*, 1992, Minamino & Macnab, 1999). Recently it has been shown that filament assembly in C-ring mutants is possible in a small fraction of the population upon overexpression of the T3S-specific ATPase FliI (Konishi *et al.*, 2009).

The assembly of the flagellum is a highly regulated process. In *Salmonella enterica* and *Escherichia coli*, the flagellar regulon is controlled by a transcriptional hierarchy of three promoter classes for the expression of more than 30 structural and assembly-related proteins (Figure 1A) (Chevance & Hughes, 2008). At the top of the transcriptional hierarchy stands the class 1 promoter for transcription of the flagellar master operon, *flhDC*. Many different signals influence expression of the class 1 promoter to ultimately determine the level of flagellar gene expression. In *S. enterica*, six transcriptional start sites have been mapped within the *flhDC* promoter region (Yanagihara *et al.*, 1999). The *flhDC* operon encodes the $FlhD_4C_2$ activator complex (Liu & Matsumura, 1994, Wang *et al.*, 2006), which directs $\sigma^{70}$-bound RNA polymerase to initiate transcription from class 2 promoters.

Class 2 gene products are required for the structure and assembly of the hook-basal body (HBB), which includes the T3S apparatus. Class 2 promoters also direct transcription of regulatory proteins such as the flagellum-specific σ-factor, $\sigma^{28}$ (Ohnishi *et al.*, 1990) and its cognate anti σ-factor, FlgM (Hughes *et al.*, 1993). Upon completion of the HBB, substrate specificity of the flagellar-specific T3S system is switched from rod-hook substrate specificity to the secretion of late substrates like the filament subunits and the anti σ-factor FlgM. FlgM secretion after HBB completion releases $\sigma^{28}$ to interact with RNA polymerase and activate transcription from class 3 promoters. Class 3 promoters control expression of late flagellar substrates like the filament subunits, the motor force generators (MotA and MotB) and the chemosensory system, but only in coordination with hook-basal body completion (Chevance & Hughes, 2008).

As mentioned above, many environmental signals are integrated on the level of the *flhDC* class 1 promoter to control the initiation or cessation of flagellar synthesis in *S. enterica*. Binding of the cyclic AMP-catabolite gene activator protein (CAP) complex to the *flhDC* promoter is required to activate transcription of *flhDC* (Komeda *et al.*, 1976, Soutourina *et al.*, 1999, Kutsukake, 1997). The iron-regulatory protein Fur, Fis and H-NS also activate *flhDC* transcription. Fis in *S. enterica* and Fur/H-NS in *E. coli* were shown to bind directly to the *flhDC* promoter (Kelly *et al.*, 2004, Soutourina et al., 1999, Stojiljkovic *et al.*, 1994). Another transcriptional regulator, SlyA that is required for virulence in *Salmonella* (Libby *et al.*, 1994), has been shown to enhance flagellin expression (Spory *et al.*, 2002).

Expression of *flhDC* is negatively regulated at both transcriptional and post-transcriptional levels by many other regulatory proteins. The RcsB regulator binds to the RcsAB box located within the *flhDC* promoter to inhibit motility (Wang *et al.*, 2007). The RcsCDB system senses several external signals, like high osmolarity, desiccation and low temperature with high zinc concentrations (Majdalani & Gottesman, 2005). FimZ, a response regulator that activates type 1 fimbrial genes, inhibits motility by affecting class 1 gene expression (Clegg & Hughes, 2002). Similarly, the PefI/SrgD complex, which activates the fimbrial

genes encoded on the *S. enterica* virulence plasmid, inhibits *flhDC* trancription in *Salmonella* (Wozniak *et al.*, 2008). In *E. coli*, the LysR-type DNA-binding protein LrhA has been identified as another negative regulator of *flhDC* transcription that directly binds to the *flhD* promoter and thereby inhibits transcription (Lehnen *et al.*, 2002). The binding of RtsB, another pathogenesis-related DNA-binding protein, also inhibits transcription of the class 1 *flhDC* promoter (Ellermeier & Slauch, 2003). EcnR, an uncharacterized regulatory protein was also identified as a novel negative regulator of class 1 transcription in *S. enterica* (Wozniak et al., 2008). Finally, deficiencies of guanosine tetraphosphate and guanosine pentaphosphate (ppGpp(p)) and the RNA-polymerase binding protein DksA respectively, have divergent effects on flagellar gene expression and motility (Aberg *et al.*, 2009).

Following transcription, the RNA-binding protein CsrA, which is also involved in carbon storage regulation, stabilizes the *flhDC* transcript (Wei *et al.*, 2001). The c-di-GMP-related protein YdiV negatively regulates $FlhD_4C_2$ activity on class 2 promoters at a post-transcriptional level (Wozniak et al., 2008). The $FlhD_4C_2$ complex is also degraded by the ClpXP protease (Tomoyasu *et al.*, 2003) and the formation of active $FlhD_4C_2$ complex is promoted by the Hsp70 chaperone DnaK (Takaya *et al.*, 2006).

In this work we sought mutants that allowed secretion of the flagellar hook protein fused to a β-lactamase reporter (deleted for its N-terminal Sec-dependent secretion signal) (FlgE-Bla) in strains defective in C-ring formation (Δ*fliMN*). We have shown previously that in strains deleted for flagellar rod genes (Δ*flgBC*), FlgE-Bla is efficiently secreted into the periplasm by the flagellar type III secretion system where it confers ampicillin resistance ($Ap^R$) (Lee & Hughes, 2006, Paul et al., 2008). Here we show that a Δ*flgBC* Δ*fliMN* double mutant will not secrete FlgE-Bla and the cells are $Ap^S$. Mutants able to secrete FlgE-Bla in the Δ*flgBC* Δ*fliMN* double mutant background ($Ap^R$) resulted in increased *flhDC* expression and HBB production supporting a role of the C-ring as an affinity cup that enhances the efficiency and specificity of flagellar T3S.

## Results

### Duplications of the *flhDC* operon overcome inhibition of FlgE-Bla secretion in a Δ*fliMN* C-ring mutant strain

For selective and quantitative measurement of flagellar T3S, we developed a reporter system consisting of the flagellar T3S-specific substrate FlgE (hook protein) fused to β-lactamase lacking its own Sec-dependent secretion signal (FlgE-Bla) (Lee & Hughes, 2006, Paul et al., 2008). In a mutant strain lacking the proximal rod subunits FlgB and FlgC, the hook-β-lactamase fusion protein is secreted into the periplasm conferring resistance to β-lactam antibiotics, like ampicillin (Figure 1B). Since the FlgE-Bla fusion protein is selectively secreted via the flagellar-specific T3S system, this powerful model system enables us to positively select for mutants with enhanced T3S by growth on otherwise inhibitory ampicillin concentrations. As mentioned earlier, the components of the cytoplasmic C-ring, FliG, FliM and FliN are needed for efficient T3S under wildtype conditions. In order to isolate mutants that allowed for secretion in the absence of the C-ring, overnight cultures of strain TH12470 (Δ*flgBC* Δ*fliMN flgE-bla*) were plated onto MacConkey ampicillin (15 ug/ml) selective medium. Ampicillin resistant ($Ap^R$) revertants arose at a frequency of ~$10^{-5}$. This high frequency of reversion suggested that loss-of-function mutations in one or more genes would allow FlgE-Bla secretion in the Δ*fliMN* mutant strain.

We performed T-POP transposon mutagenesis in an attempt to isolate insertions that resulted in FlgE-Bla secretion in a rod-defective (Δ*flgBC*), C-ring-defective (Δ*fliMN*) strain by screening insertion mutants for those that resulted in an $Ap^R$ phenotype. T-POP transposons are derivatives of the mini-Tn*10* transposon Tn*10d*Tc that encodes tetracycline

resistance ($Tc^R$) (Lee *et al.*, 2007, Rappleye & Roth, 1997). The T-POP transposon used, Tn*10d*Tc[Δ25], is a Tn*10d*Tc derivative that lacks Tn*10* transposase and is deleted for the transcriptional terminator of the tetracycline resistance gene, *tetA*, within the transposon (the [Δ25] deletion). The divergently transcribed *tetA* and *tetR* gene encode an inner membrane efflux pump (TetA) and the TetR repressor of *tetA* and *tetR* transcription. When tetracycline (Tc) is present, it will bind to TetR and prevent DNA binding resulting in de-repression of the *tetA* and *tetR* genes. Some of the *tetA* and *tetR* transcripts will continue into adjacent chromosomal DNA flanking a Tn*10d*Tc insertion. When Tc is added to strains that carry the Tn*10d*Tc[Δ25] T-POP insertion, a substantial amount of transcription from the *tetA* promoter will continue into adjacent chromosomal DNA flanking the site of T-POP insertion (Rappleye & Roth, 1997).

The T-POP transposon was introduced into strain TH14953 (pNK2880Km/Δ*flgBC* Δ*fliMN flgE-bla*), which constitutively expresses a mutant Tn*10* transposase from plasmid pNK2880Km. The mutant Tn*10* transposase has lost target specificity and catalyzes random transposition into the chromosome by P22 transduction selecting for $Tc^R$ and screening for $Ap^R$ in the presence and absence of Tc. Of 24,000 $Tc^R$ insertions, 91 were isolated that showed an $Ap^R$ phenotype: 32 were $Ap^R$ with or without added Tc, 23 were $Ap^R$ only with added Tc and 36 were $Ap^S$ when Tc was added to the medium. This is an unusually high mutation rate. The *S. enterica* chromosome has about 5000 genes. Assuming to the first approximation that the T-POP transposon inserts with an equal frequency in any given gene, 91/24,000 suggests a target of 18 genes that, when mutated, result in an $Ap^R$ phenotype. During the handling of the $Ap^R$ T-POP insertions, nine of the mutants segregated $Tc^S$ $Ap^S$ colonies at a high frequency (>10% from an overnight culture) when Tc and Ap were absent from the medium. Since duplication of that region of the chromosome was reported to occur at a frequency of $\sim 10^{-4}$ (Anderson & Roth, 1978), these observations led us to conclude that $Ap^R$ was occurring at a high frequency, independent of transposon mutagenesis by chromosomal duplications.

In order to test whether chromosomal duplications were giving rise to $Ap^R$ in the Δ*flgBC* Δ*fliMN flgE-bla* background, Mu*dJ* transposon mutagenesis was performed on strain TH12470 (Δ*flgBC* Δ*fliMN flgE-bla*) to isolate insertions in duplicated regions that result in $Ap^R$. These would have the phenotype of losing the Mu*dJ* transposon at a high frequency when selection for maintaining the duplication is removed by growing these strains without added Ap to the medium. Mu*dJ* transposon mutagenesis was performed on strain TH12470 selecting for kanamycin resistance ($Km^R$) in the presence of bromo-chloro-indolyl-galactopyranoside (XGal). The Mu*dJ* is a *lac* operon fusion vector. When Mu*dJ* inserts into a gene in the correct orientation the promoter of the inserted gene will transcribe promoterless *lac* operon within Mu*dJ*. We screened for $Ap^R$ Mu*dJ* insertion mutants that showed an initial $Lac^+$ phenotype in the presence of XGal (= blue colony), but upon restreaking on XGal medium lacking both Ap and Km segregated $Lac^-$ (white on XGal) colonies. This indicated that the Mu*dJ* had inserted within a duplicated region. A number of the unstable (duplication-held) $Ap^R$ Mu*dJ* insertions were analyzed by DNA sequencing. As shown in Figure 2 and Table 1, these Mu*dJ* insertions were in a number of unrelated genes yet they localized to a region of the chromosome that includes the *flhDC* operon, suggesting that duplication of the region of the chromosome that includes *flhDC* resulted in the $Ap^R$ phenotype. To verify this possibility, C-ring deletions strains (Δ*fliMN*, Δ*fliG* and Δ*fliGMN*), as well as deletions of the MS-ring (Δ*fliF*) and the ATPase complex (Δ*fliHIJ*) were constructed with an extra copy of the *flhDC* expressed from the arabinose promoter. Expression of *flhDC* from the arabinose promoter will provide about 60-fold more copies of *flhDC* mRNA than *flhDC* expressed from its native promoter (Figure 3B), however it has been shown previously that duplications tend to amplify to many more copies as well depending on selection (Kugelberg *et al.*, 2006).

In the strain expressing *flhDC* from the arabinose promoter, the C-ring deletion strains were $Ap^R$ in the presence of arabinose and $Ap^S$ without added arabinose confirming that an at least two-fold excess *flhDC* was sufficient to allow FlgE-Bla secretion in the C-ring defective strain (Figure 3A). The strain deleted for the ATPase complex FliHIJ was also $Ap^R$ in the presence of arabinose, confirming previous results that the ATPase function is not necessary for flagellar type III secretion (Paul et al., 2008, Minamino & Namba, 2008). While efficient secretion is possible under excess FlhDC in both the absence of the C-ring or ATPase complex, the deletion of the MS-ring prevented secretion. This indicates that the MS-ring has an essential function as a scaffold harboring the secretion apparatus, but the requirement of the C-ring and the ATPase complex can be overcome by excess substrate concentrations and increased number of potential secretion systems (see below).

It is important to note that the expression of *flhDC* from the arabinose promoter resulted in an about 60-fold upregulation of *flhDC* transcript levels if compared to wildtype *flhDC* expression (Figure 3B). However, different arabinose (0%, 0.05%, 0.2% and 0.6%) did neither change *flhDC* mRNA levels, nor upregulated Class 2 gene expression further than 4–5 fold. As shown below, consensus -10 box mutations of the *flhD* promoter result in only two-fold upregulation of *flhDC*, as well as Class 2 gene expression (Figure 6C). However, this change is sufficient to allow for efficient type III secretion in the absence of the C-ring. This indicates that activation of Class 2 gene expression by the $FlhD_4C_2$ complex is saturated early by only a small increase in *flhDC* levels an cannot be increased further. Importantly, this result explains why already a small increase in *flhDC* expression (e.g. a $P_{flhD}$ promoter up mutation or duplication of the *flhDC* operon) is sufficient to bypass the C-ring deletion.

## Characterization of T-POP insertions that allow hook-β-lactamase (FlgE-Bla) secretion in the absence of the C-ring

DNA-sequence analysis was performed on 42 independent $Ap^R$ T-POP insertions in the Δ*flgBC* Δ*fliMN flgE-bla* background that did not appear to contain a duplication (they did not segregate $Ap^S$ $Tc^S$ segregants in the absence of selection) (Figure 4 and Table 2). Most T-POP transposon insertions resulted in an increase in FlhDC activity, by either downregulation of known transcriptional and post-transcriptional inhibitors of FlhDC (e.g. FliT, LrhA, ClpP) or upregulation of the *flhDC* operon itself (e.g. insertions in the *flhDC* promoter that increase *flhDC* expression).

Initially, the $Ap^R$ T-POP mutants fell into three phenotypic classes (Table 2). (i) The first class of mutants was $Ap^R$ solely by the T-POP insertion, indicating that the insertion knocked-out a gene whose product negatively influenced flagellar T3S in the absence of the C-ring ($Ap^R$::T-POP). (ii) The $Ap^R$ phenotype of the second class of mutants was dependent on addition of tetracycline, indicating that the transcriptional read-through from the *tetA* promoter induces expression of an adjacent gene that positively influences flagellar T3S in the absence of the C-ring (Tc-$Ap^R$). Alternatively, the transcriptional read-through from the *tetA* promoter could produce antisense RNA that would impair expression of adjacent genes. (iii) The last class of $Ap^R$ mutants displayed an $Ap^S$ phenotype in the presence of tetracycline (Tc-$Ap^S$). In this case the induction of *tetA* by addition of tetracycline presumably induces the expression of genes that negatively influence flagellar T3S in the absence of the C-ring.

In summary, we isolated three $Ap^R$::T-POP insertions in the promoter region of *flhDC* that potentially disrupt binding sites of negative regulators of *flhDC* transcription. Three more T-POP insertions in the *flhDC* promoter displayed a Tc-dependent $Ap^R$ phenotype (Tc-$Ap^R$), indicating an overexpression of *flhDC* upon Tc addition (Figure 4). Two $Ap^R$::T-POP, one Tc-$Ap^R$ and one Tc-$Ap^S$ T-POP transposon insertion were in the coding region or promoter

of *fliD* respectively (Figure 4). The transposon insertions in *fliD* presumably resulted in a polar effect on the expression of *fliT*, an anti-$FlhD_4C_2$ factor that prevents binding of the activator complex to class 2 promoters (Yamamoto & Kutsukake, 2006). This was verified by the introduction of a *fliT* deletion allele into strain TH12470 (Δ*flgBC* Δ*fliMN flgE-bla*), which resulted in an $Ap^R$ phenotype. Additionally, we isolated T-POP insertions in known negative regulators of *flhDC* transcription or FlhDC levels, like *lrhA*, *ecnR*, *rcsB*, *ydiV* and *clpP*. Null alleles of these inhibitor loci presumably resulted in increased *flhDC* expression or increased stability of the $FlhD_4C_2$ activator complex. Accordingly, we isolated five T-POP insertions in the coding region or vicinity of *lrhA*, a LysR-type DNA-binding protein that was previously characterized as a regulator of *flhDC* transcription in *E. coli* (Lehnen et al., 2002) (Figure 4). One Tc-$Ap^S$ T-POP insertion was found in the coding region of *ecnR*, a recently characterized regulator of flagellar gene expression (Wozniak et al., 2008). Another Tc-$Ap^S$ T-POP insertion had been inserted in *yjek*, downstream of *ecnR*, thereby presumably negatively influencing the expression of *ecnR* (Figure 4). One $Ap^R$::T-POP transposon had inserted in the coding region of *slyA*, a DNA-binding protein that has been previously shown to enhance expression of filament subunits (Spory et al., 2002). Two $Ap^R$::T-POP transposons were isolated in the coding region of *rcsB* and one Tc-$Ap^S$ transposon had inserted in *rcsD* (*jojN*), upstream of *rcsB* (Figure 4). RcsB is another negative regulator of *flhDC* expression and has been shown to directly bind the *flhD* promoter (Wang et al., 2007). We isolated one Tc-$Ap^S$ T-POP insertion in the promoter region and two T-POP insertions (one $Ap^R$::T-POP and one Tc-$Ap^S$ T-POP) in the coding region of the c-di-GMP-related protein YdiV (Figure 4). YdiV negatively regulates $FlhD_4C_2$ activity at a post-transcriptional level (Wozniak et al., 2008). One Tc-$Ap^S$ T-POP transposon had inserted in the coding region of *clpP*. It has been previously shown that the $FlhD_4C_2$ complex is degraded by the ClpXP protease (Tomoyasu et al., 2003).

T-POP insertions isolated in the promoter region of the *fliAZ* operon showed opposite effects: two were Tc-$Ap^R$ and one was Tc-$Ap^S$ (Figure 4). The *fliZ* gene encodes an activator of *flhDC* (Saini *et al.*, 2008) and the SpiI virulence system. The *fliA* gene encodes $\sigma^{28}$, which inhibits *flhDC* transcription (see below). Thus, these insertions could affect *fliA*, *fliZ* or both. We also isolated two $Ap^R$::T-POP transposon insertions in the coding region of *flgM* and promoter region of *flgA*, upstream of *flgM*, respectively. Insertions in *flgA* are polar on *flgM* transcription. Kutsukake (Kutsukake, 1997) showed that the *flhD* operon is autogenously repressed in the presence of both $\sigma^{28}$ and its cognate anti-sigma factor FlgM. However, *flhDC* expression is activated in the presence of $\sigma^{28}$ and the absence of FlgM. As shown in Figure 5D, the overproduction of *fliA* from the arabinose promoter results in inhibition of *flhC* transcription in a strain harboring a functional copy of the *flgM* gene. This unknown mechanism of *flhDC* regulation would explain the effects on *flhDC* expression by our T-POP insertions in both *flgM* and the promoter region of the *fliAZ* operon.

Additionally, we isolated twelve T-POP transposon insertions in genes that are not obviously related to *flhDC* regulation. One $Ap^R$::T-POP insertion was located after bp 608 of the 795 bp *fliR* gene. Two T-POP had inserted into the vicinity of *sopE2*, a type III-secreted effector protein. Two more Tc-$Ap^R$ T-POP insertions were located to the coding region or vicinity of STM2011, a protein of unknown function. Seven more single T-POP insertions were found to be in *rfbP* (undecaprenol-phosphate galactosephosphotransferase/ O-antigen transferase), *pgtE* (outer membrane protease), *ddg/yfdZ* (lipid A biosynthesis palmitoleoyl-acyltransferase and aminotransferase), *pykF* (pyruvate kinase), *garL* (alpha-dehydro-beta-deoxy-D-glucarate aldolase), *yieP* (putative regulatory protein) and *hpaX* (4-hydroxyphenylacetate permease) respectively. Each will require further characterization to determine how they result in $Ap^R$.

### Effects of T-POP insertions on flagellar gene transcription

T-POP insertions in *fliD* presumably have a polar effect on *fliT*, a negative regulator of *flhDC*. Accordingly, we analyzed Class 2 transcription in various T-POP insertions that resulted in an $Ap^R$ phenotype in the absence of the C-ring components FliM and FliN (Figure 5A). We found that the T-POP insertions in *fliD*, *fliD7879* and *fliD7881* respectively increased Class 2 transcription about 20 – 30%. T-POP insertions in the coding region of *lrhA*, *slyA* and *ecnR* had the most pronounced effect on Class 2 transcription. The loss-of-function T-POP insertion in *lrhA2* increased Class 2 transcription about 1.7 fold, whereas the T-POP insertions in *slyA* and *ecnR* allowed for 1.3 – 1.4 fold enhanced Class 2 transcription.

Several other analyzed T-POP insertion had no apparent effect on Class 2 transcription, although the insertions resulted in an $Ap^R$ phenotype in the C-ring deletion mutant. Surprisingly, the induction of down-and upstream genes of the respective T-POP insertions by induction with tetracycline, resulted in 10 – 30% decreased Class 2 transcription in the cases of *ecnR7* (insertion in *yjek*, upstream of *ecnR*), STM1856, *ddg/yfdZ1* and STM2011 (Figure 5A). We therefore asked the question whether the Tc-$Ap^S$ phenotype of the *ecnR7*::T-POP (insertion in *yjek*, upstream of *ecnR*) was due to Tc-dependent induction of *ecnR*. Accordingly, we analyzed *ecnR* transcription using a *ecnR*::Mu*dJ* (*lac* transcriptional fusion) insertion described previously (Wozniak et al., 2008). As shown in Figure 5B, the T-POP insertion in *yiek* (*ecnR7*) displayed no apparent defect in *ecnR* transcription in the presence or absence of tetracycline.

Also, the effects of other T-POP insertions in less characterized genes or in intergenic regions remain elusive so far. Those T-POP insertions might confer $Ap^R$ in the C-ring deletion mutant by the means of other mechanisms unrelated to regulation of *flhDC*. Possible reasons that would allow for elevated FlgE-Bla secretion include an increased proton-motive force gradient, less competition between secretion substrates or effects on localization of type III secretion substrates.

In conclusion, most of the analyzed T-POP insertions directly affect negative regulators of *flhDC*, thus resulting in increased Class 2 transcription and accordingly in enhanced secretion substrate levels. If the C-ring functions as an affinity cup that increases the efficiency of the secretion process, then elevated levels of substrates, like the hook-β-lactamase protein would still allow for sufficient secretion to confer $Ap^R$.

### LrhA and SlyA negatively regulate *flhDC* transcription in *Salmonella enterica*

In our screen for mutants that allowed flagellar type III secretion in the absence of the C-ring, we isolated several T-POP insertions in two previously uncharacterized regulatory loci of *flhDC* expression in *S. enterica*, *lrhA* and *slyA* (Table 2). The LysR-type regulator LrhA has been previously shown to negatively regulate transcription of *flhDC* in *E. coli* (Lehnen et al., 2002). Conversely, the lack of the DNA-binding protein SlyA has been associated with increased flagellin expression (Spory et al., 2002). To analyze the effects of LrhA and SlyA in *Salmonella*, we cloned both putative regulators under the control of the arabinose promoter. As shown in Figure 5C, the expression of LrhA and SlyA respectively from the arabinose promoter decreases *flhDC* transcription 40 – 60%. Therefore, we conclude that both LrhA and SlyA act as negative regulators of *flhDC* transcription in *S. enterica*.

### Null alleles in *fliA* and *flhDC* promoter mutants result in FlgE-Bla secretion in the absence of the C-ring

We attempted to isolate amino acid substitutions in flagellar genes that resulted in FlgE-Bla secretion in strains missing part (Δ*fliMN*) or all (Δ*fliG*) of the C-ring. Using the FlgE-Bla

reporter construct in the rod-minus mutant background described above, we used transposons linked to the *flh* and *fli* flagellar regions to separate *flh*- and *fli*-linked $Ap^R$ mutants from mixed pools of spontaneous $Ap^R$ colonies. Spontaneous $Ap^R$ mutants arose in strain TH12470 (Δ*flgBC flgE-bla*Δ*fliMN*) at a frequency of $10^{-5}$ and in strain TH12466 (Δ*flgBC flgE-bla*Δ*fliG*) at a frequency of $10^{-8}$. A *mutS*::Km insertion was introduced into strain TH12466 and the frequency of spontaneous $Ap^R$ mutants rose to $10^{-6}$. In the Δ*fliG* strain the complete C-ring is missing since FliG acts as a scaffold for FliMN assembly, whereas in the Δ*fliMN* strain two-thirds of the C-ring is not assembled. The lower frequency of mutation in the Δ*fliG* strain compared to the Δ*fliMN* strain can be explained by the following: 1) the physical C-ring structure may have importance in providing affinity sites for substrates or excluding non-substrates or 2) FliG in addition to FliMN provides additional interaction sites for secretion substrates. Accordingly, if the whole structure is missing (Δ*fliG*), one would expect a more pronounced effect than if two-thirds are missing (Δ*fliMN*). Additionally, we showed above that Δ*fliMN* displays increased FlgE-Bla secretion under excess FlhDC conditions compared to both Δ*fliG* and Δ*fliGMN*, where the complete C-ring is missing (Figure 3A). These results provide important evidence for our model of the C-ring acting as an affinity cup-like structure that locally increases secretion substrate concentration prior to secretion or excludes non-substrate interactions as discussed below.

Individual mutants that were linked to the *flhDC* operon were isolated in the Δ*fliMN* and Δ*fliG* backgrounds. DNA sequence analysis showed them to be single base pair changes in the *flhD* promoter region: *−368G:A* (relative to AUG start codon) in the Δ*fliG* background and *−152C:T* in the Δ*fliMN* background). The *−368G:A* allele changed the -10 sequence for the P4 promoter toward the consensus -10 $\sigma^{70}$ binding site from TGGAAT to TAGAAT and the *−152C:T* allele change was outside any known promoter region, but presumably allowing for increased *flhDC* expression by affecting the binding site of a negative regulator of *flhDC* expression (Table 2). Two mutations that mapped to the *fliAZY* operon were both single base pair changes resulting in nonsense mutations of the *fliA* gene (Q106Stop, Table 2). This suggested that loss of $\sigma^{28}$-dependent transcription increased FlhDC activity. We tested for the effect of increased *fliA* gene expression on an *flhC*::Mu*dJ* reporter construct by over-expression of a second copy of *fliA* gene from the arabinose promoter. If the loss of $\sigma^{28}$-dependent transcription would increase FlhDC activation of class 2 promoters, then increased *fliA* expression should have a negative effect on *flhDC* expression. As shown in Figure 5D, the addition of arabinose resulted in the inhibition of *flhDC* transcription. This result is an apparent contradiction to our earlier results that showed increased *flhDC* activity, as measured by FlgE-Bla secretion in the Δ*flgBC* Δ*fliMN* background in strains with reduced FlgM levels. One would expect that reduced FlgM levels result in increased $\sigma^{28}$ activity, which in turn should negatively influence *flhDC* expression as described above. However, these results are consistent with previous results from K. Kutsukake (Kutsukake, 1997) who showed that the *flhDC* operon was autogenously repressed, except under the condition where *flgM* was inactivated in a *fliA*$^+$ background. In the *flgM*-defective *fliA*$^+$ background the *flhDC* operon was autogenously activated (Kutsukake, 1997). These apparent conflicting results of $\sigma^{28}$-dependent inhibition of *flhDC*, and FlgM (anti-$\sigma^{28}$)-dependent inhibition of *flhDC* warrant further study. It is possible that the FlgM/$\sigma^{28}$ complex acts directly or indirectly to inhibit *flhDC* transcription.

### Effects of *flhDC* perfect -10 box promoter mutants on swimming motility and HBB number

Based on the discovery that single base pair changes in the *flhD* promoter are sufficient to allow for flagellar type III secretion in the absence of the C-ring, we further characterized the effects of *flhD* promoter mutants. The *flhDC* operon is transcribed from at least 6 different promoters and we constructed mutations in the known P1, P2, P3, P5 and P6 *flhD* promoter sequences to have a consensus -10 box (TATAAT) (Supplemental Figure 2). As

shown in Figure 6A, the perfect -10 box mutations of the P3, P5 and P6 promoter had no apparent effect on swimming motility. However, the mutation of the P1 promoter resulted in an apparent 1.7 fold increased migration rate in the swim plate compared to the wildtype (Figure 6A and 6B). The combination of $P_{flhDC}$ P1 and P4 -10 box mutations did not further increase motility, whereas the perfect -10 box mutation of the P2 promoter decreased motility to about 50% of wildtype motility (Figure 6A and 5B). In order to further characterize the effects of the $P_{flhDC}$ promoter mutations on flagellar gene expression, we performed real-time quantitative PCR analysis of cDNA reversely transcribed from strains harboring the $P_{flhDC}$ P1 or the $P_{flhDC}$ P2 perfect -10 box mutation. As displayed in Figure 6C, the P1 mutation resulted in an about 2-fold upregulation of *flhDC* mRNA, whereas the P2 mutation resulted in a slight downregulation of *flhDC* mRNA levels. We additionally confirmed this finding using an *flhC-lac* fusion construct (data not shown). On the level of class 2 and class 3 flagellar genes expression, the P1 and P2 -10 box mutations also resulted in an up- or downregulation respectively (Figure 6C). In case of the P1 mutation, *flgE* expression is enhanced about 2-fold, whereas *flgE* expression in the P2 mutant is slightly decreased. Similarly, the mRNA levels of the motor force generator proteins MotAB are upregulated more than 2-fold in the P1 mutant and downregulated in the P2 mutant background (Figure 6C). Taken together, the increase in *flhDC* expression results in an about 2 – 4 fold increase in flagellar class 2 and class 3 gene expression that explains the differences in motility described above. To confirm the 2-fold upregulation of hook-basal-body (HBB) type secretion substrates on a protein level, we examined expression of the hook-β-lactamase fusion construct in the $P_{flhDC}$ P1 perfect -10 box mutation background by quantitative Western blot analysis. As shown in Figure 6D, FlgE-Bla is upregulated about 1.6 fold in the P1 promoter mutant.

Accordingly, every mutation that resulted in an increase in $FlhD_4C_2$ levels resulted in an about 2-fold upregulation of both structural components of the hook-basal-body complex, as well as HBB-type secretion substrates.

Based on the upregulation of HBB-type substrates we next investigated whether the number of hook-basal-bodies per cell is also increased. For this we utilized an FlgE variant harboring a hemagglutinin (HA) epitope tag for specific and sensitive immunodetection of completed hook-basal-body structures. We additionally used GFP fusions to components of the C-ring, FliM and FliG respectively, to analyze assembled C-rings by fluorescent microscopy. As shown in Figure 7A, the number of completed hook-basal-bodies per cell under wildtype *flhDC* levels peaks at about 2 HBB per μM cell length. Accordingly, wildtype *S. enterica* produces about 4 – 6 hook-basal-body structures per cell. We next investigated the effects of both the $P_{flhDC}$ P1 perfect -10 box mutation and the combination of the P1 + P4 perfect -10 box mutation on the number of hook-basal-body structures per cell. As displayed in Figure 7B and 7C, the number of HBBs doubles to about 4 HBBs per μM cell length in either the P1 or the P1 + P4 combination mutant. The $P_{flhDC}$ P1 perfect -10 box mutant therefore effectively doubles the number of available secretion systems (= HBBs) per cell, which is consistent with the gene expression data mentioned earlier. The number of completed HBBs in the $P_{flhDC}$ P2 perfect -10 box mutant however, are greatly reduced (Figure 7D). The majority of the cells do not complete a HBB, which might provide an explanation for the severe reduction in motility as shown in Figure 6A and 6B.

We additionally confirmed the 2-fold upregulation of flagellar basal body structures using FliG-GFP and FliM-GFP protein fusions mentioned above (Supplemental Figure 1A and 1B). By overexpressing functional *flhDC* from the inducible arabinose promoter ($P_{araB}$-$flhD^+C^+$) we could furthermore confirm that elevated $FlhD_4C_2$ levels and thus increased expression of class 2 genes produces about 2-fold more HBB structures per cell compared to wildtype *flhDC* levels (Supplemental Figure 1C).

In summary, these data demonstrate that the upregulation of *flhDC* expression increases both the availability of secretion substrates and the number of export systems *per se* and taken together, these effects account for flagellar type III secretion even in the absence of the C-ring.

## Discussion

In this work we employed a random screen for enhanced flagellar type III-specific protein secretion in a secretion deficient C-ring deletion mutant using the T-POP transposon. We utilized a hook-β-lactamase (FlgE-Bla) fusion construct in a strain deleted for the rod proteins FlgB and FlgC to positively select for flagellar type III secretion. The hook-β-lactamase reporter protein is selectively secreted via the flagellar T3S apparatus located at the base of the hook-basal-body and confers ampicillin resistance if secreted into the periplasm in a strain missing the proximal rod subunits FlgB and FlgC (Lee & Hughes, 2006). In a strain deleted for two thirds of the cytoplasmic C-ring (Δ*fliMN*), flagellar T3S is severely impaired and the FlgE-Bla reporter remains in the cytoplasm. Using a random T-POP transposon mutagenesis approach, we positively selected for T-POP transposon insertions that allowed for FlgE-Bla secretion even in the absence of the C-ring.

We isolated and analyzed by DNA-sequencing 42 independent T-POP insertions that we grouped into three different classes. The first class of T-POP insertions conferred ampicillin resistance without induction of the down- or upstream genes using tetracycline ($Ap^R$::T-POP). The second class of mutants conferred ampicillin resistance after induction of down- or upstream genes using tetracycline (Tc-$Ap^R$). The mutants where induction with tetracycline resulted in an ampicillin sensitive phenotype were grouped into the third class of T-POP insertions (Tc-$Ap^S$). In summary, we obtained $Ap^R$::T-POP insertions in the coding region of several negative regulators of *flhDC*, e.g. *lrhA, slyA, ydiV, rcsB, ecnR* and *clpP*. Those proteins have been previously shown to regulate *flhDC* expression or $FlhD_4C_2$ protein stability in *E. coli* or *S. enterica*. We additionally isolated several T-POP insertion in *fliD*, upstream of *fliT*, another negative regulator of *flhDC*. In a complimentary approach, we selected Mu*d* insertions in the *Salmonella* chromosome that conferred ampicillin resistance in the absence of the C-ring by duplication of the *flhDC* operon. We confirmed this finding by expressing a second copy of *flhDC* from the arabinose promoter. Mutant strains (Δ*flgBC flgE-bla* $P_{ara}$-*flhD*$^+$*C*$^+$) missing two-thirds (Δ*fliMN*) or the complete C-ring (Δ*fliG* and Δ*fliGMN*) were found to be $Ap^R$ in the presence of arabinose, but not without. Importantly, excess FlhDC also allows for efficient secretion in a Δ*fliHIJ* deletion mutant, confirming the previous finding that the ATPase complex FliHIJ is not needed for flagellar type III secretion *per se* (Paul et al., 2008, Minamino & Namba, 2008). Additionally, we obtained several spontaneous mutants of the *flhD* promoter region that conferred ampicillin resistance, as well as non-sense mutations in *fliA*. The sigma-factor $\sigma^{28}$ has been shown to repress *flhDC* transcription in the presence of its cognate anti-sigma factor FlgM (Kutsukake, 1997). Additionally, $\sigma^{28}$ activates the expression of negative regulators of *flhDC*, like FliT. Accordingly, the non-sense mutation of *fliA* allows for increased *flhDC* expression, which in turn confers ampicillin resistance using the same mechanism proposed below.

We analyzed several T-POP insertions for their effects on class 2 gene expression and found an increased class 2 expression by the T-POP insertions in *lrhA*, *slyA* and *fliD*. We additionally demonstrated that both LrhA and SlyA act as negative regulators of *flhDC* expression in *S. enterica*. LrhA (Lehnen et al., 2002) and SlyA (Spory et al., 2002) have been previously shown to act as regulators of *flhDC* and *fliC* respectively in *E. coli*.

In summary, we identified by our T-POP mutagenesis approach several known regulatory loci of flagellar Class 1 gene expression in *S. enterica*, like *ecnR* (Wozniak et al., 2008), *ydiV* and *rcsB* (Wang et al., 2007). We showed that both LrhA and SlyA act as negative regulators of *flhDC* expression also in *S. enterica*. We additionally identified several putative regulators of Class 2 transcription like STM1856 and STM2401/STM2402. A summary of the regulatory network influencing Class 1 gene expression is given in Figure 8A. Taken together we conclude that the upregulation of *flhDC* expression by impairing the function of the above mentioned negative regulators of *flhDC* expression is sufficient to answer the selective pressure of our FlgE-Bla secretion assay in the absence of the C-ring.

To further analyze the effects of *flhDC* upregulation, we designed several *flhD* -10 box promoter mutants (Supplemental Figure 2). Using those mutants we demonstrate that single base pair changes in the P1 *flhD* promoter result in a significant upregulation of *flhDC* gene expression. The increased expression of *flhDC* results in 2 – 4 fold increase in class 2 and class 3 gene expression and additionally in an about 2-fold increased migration rate as analyzed using motility plates. The enhanced class 2 gene expression also translates in an almost 2-fold increase in protein levels of the reporter protein FlgE-Bla as analyzed by quantitative Western blotting. Interestingly, *Salmonella* cells harboring the perfect -10 box mutation of the P1 *flhD* promoter produce about 2 fold more HBB per cell if compared to cells expressing wildtype *flhDC* levels. A perfect -10 box mutation of the P2 *flhD* promoter however, resulted in a decrease of class 1, class 2 and class 3 gene expression, as well as in significantly reduced number of HBB per cell as analyzed by fluorescent microscopy. It was surprising to find that just a two-fold increase in the level of *flhDC* mRNA can circumvent the impaired secretion activity caused by the absence of the C ring. It suggests that the role of the C-ring as the rotor of the flagellar motor is its primary function and the C-ring plays only a minor role in the secretion process as an affinity site for substrate localization."

In summary, we propose the following mechanism for flagellar type III secretion in the absence of the C-ring by upregulation of *flhDC*: Every mutation that results in an increased level of functional $FlhD_4C_2$, like T-POP insertions in negative regulators of *flhDC* or mutations in the P1 promoter of *flhD*, will allow for FlgE-Bla secretion even in the absence of the C-ring by a combination of I) more available substrates (FlgE-Bla) and II) more potential secretion systems (more HBB complexes). Under conditions where the function of the C-ring is missing or impaired, flagellar type III secretion might still occur, albeit more inefficient, if the concentration of the secretion substrates are increased. This is the case in our isolated T-POP mutants that increase *flhDC* expression by impairing the function of negative regulators of *flhDC*, as well as in our *flhDC* promoter mutants that directly increase *flhDC* gene expression.

Accordingly, we propose that the C-ring acts under physiological conditions as an affinity cup that locally increases the secretion substrate concentration prior to type III secretion by either I) transiently binding secretion substrates or II) excluding non-secretion substrates interactions with the secretion apparatus (Figure 8B). Folded secretion substrates are bound by the cargo delivery complex FliHIJ and recruited to the C-ring affinity cup, thereby locally increasing the substrate concentration prior to secretion. Importantly, the function of the C-ring as an affinity cup in type III secretion seems to be highly conserved. Recently it has been shown that in case of the *Chlamydia* injectisome type III secretion system a multiple cargo secretion chaperone (Mcsc) bound to secretion substrates is recruited to the putative C-ring homolog CdsQ, thereby presumably allowing for a more efficient secretion process (Spaeth *et al.*, 2009).

## Experimental procedures

### Bacterial strains, plasmids and media

All bacterial strains used in this study are listed in Supplemental Table 1. Cells were cultured in either Luria broth (LB) or peptone/protease-peptone/bile-salts (PPBS) (17 g/l peptone, 3 g/l protease peoptone, 1.5 g/l bile salts #3, 5 g/l sodium chloride, 10.8 g/l agar). A concentration of 5 μg/ml ampicillin and 15 μg/ml tetracycline was used in PPBS plates. Growth of strain TH12470 harboring the hook-β-lactamase reporter protein and missing two-thirds of the C-ring (Δ*fliMN*) was inhibited on PPBS plates containing 5 μg/ml ampicillin. Motility agar plates were prepared as described before (Gillen & Hughes, 1991, Wozniak et al., 2008). The generalized transducing phage of *S. typhimurium* P22 *HT105/1 int-201* was used in all transductional crosses (Sanderson & Roth, 1983).

### SDS-PAGE and Western Blotting

Whole-cell lysates of *Salmonella* were subjected to sodium dodecyl sulfate-polyacrylamide gel electrophoresis (SDS-PAGE) and analyzed by immunoblotting using anti-FlgE antibodies (rabbit) for detection of FlgE-β-lactamase. Specific protein detection of horseradish peroxidase-conjugated secondary antibodies (Bio-Rad) was performed using ECL plus Western blotting detection reagents (Amersham Biosciences). Densitometric measurements of FlgE-β-lactamase bands were performed using ImageJ 1.42m for Mac OS X (Abramoff *et al.*, 2004).

### Isolation of random T-POP insertions spontaneous $Ap^R$ mutants that allow Hook-β-lactamase secretion in the absence of the C-ring

The screen for random Tn*10d*Tc[Δ25] transposon insertions allowing type III-specific secretion in the C-ring deletion mutant was essentially performed as described in (Wozniak et al., 2008, Lee et al., 2007) using strain TH12470 as the recipient on PPBS plates containing 5 μg/ml ampicillin.

Spontaneous mutations that conferred FlgE-Bla secretion in a C-ring deletion strain that were linked to either the *flh* or *fli* regions were isolated using transposons STM1911::Tn*10d*Tc and *zec-3521*::Tn*10d*Cm that are linked to the *flh* and *fli* regions, respectively. $Ap^R$ mutants were pooled, a phage P22 transducing lysate was grown on the pooled cells and used to transduce either a Δ*flgBC flgE-bla* Δ*fliG* (TH12466) or Δ*flgBC flgE-bla* Δ*fliMN* (TH12470) recipient to either $Tc^R$ or $Cm^R$. $Tc^R$ transductants that also inherited $Ap^R$ resulted from co-transduction of the $Ap^R$ allele with *flh*-linked STM1911::Tn*10d*Tc. $Cm^R$ transductants that also inherited $Ap^R$ resulted from co-transduction of the $Ap^R$ allele with *fli*-linked *zec-3521*::Tn*10d*Cm. Linked $Ap^R$ mutants were characterized further using three-factor crosses and the mutations were determined using DNA sequencing analysis.

### β-galactosidase assays

β-galactosidase assays were performed based on the protocol of Zhang and Bremer (Zhang & Bremer, 1995) with minor modifications. Briefly, logarithmic growing cells were permeabilized using 100 mM $Na_2HPO_4$, 20 mM KCl, 2 mM $MgSO_4$, 0.08% CTAB (hexadecyl-trimethylammonium bromide), 0.04% sodium deoxycholate and 5.4 μl/ml β-mercaptoethanol. Afterwards, the reaction was started by addition of 60 mM $Na_2HPO_4$, 40 mM $NaH_2PO_4$, 1 mg/ml o-nitrophenyl-β-D-Galactoside (ONPG) and 2.7 μl/ml β-mercaptoethanol. The reaction was stopped using 1 M Sodium Carbonate ($Na_2CO_3$) and Miller units were calculated as described (Miller, 1972). For each strain, the assay was performed using three independent, biological replicates.

### RNA isolation and quantitative real-time PCR

RNA was prepared from three independent, biological replicates essentially as described (Simm *et al.*, 2009) using the SV Total RNA Isolation System (Promega) and on-column DNase I treatment. Alternatively, cultures of three independent, biological replicates were mixed equally and used for the subsequent purification of total RNA as described above. For complete removal of genomic DNA, purified RNA samples were treated a second time with DNase I for one hour at 37 °C (ZymoResearch). Afterwards, RNA samples were reverse transcribed using the RETROscript kit and random decamers (Ambion). qPCR reactions were performed using the EvaGreen qPCR master mix (BioRad) and primers 5'-GTAGGCAGCTTTGCGTGTAG + 5'-TCCAGCAGTTGTGGAATAATATCG (*flhDC*), 5'-GAACACGTTCGCGCAGTG + 5'-TAGGCAATTTTCCAGGAACCG (*motAB*), 5'-GATGGCGGCGAAATCG + 5'-AGGGTCCGTTGAGTTCAGGTT (*flgE*), 5'-GGCCAAAGCTGGTCATTATCC + 5'-TCGCCGGCAGAAACGT (*fliP*), 5'-CGCCCTGTTGACGATCTGG + 5'-TTTACCCAAGTTAGGCGTCTTAAG (*rpoA*), 5'-CAACCTGTTCGTACGTATCGAC + 5'-CAGCTCCATCTGCAGTTTGTTG (*rpoB*), 5'-CAACAGTATGCGCGTGATGAT + 5'-CGACGCAGAGCTTCATGATC (*rpoD*), 5'-CTGCTCAAAGAGCTGGTGTATCA + 5'- AGCGCGTTACAGTCTGCTCAT (*gyrB*) and 5'-TTGCAGAAATGAGCCATTACGCCG + 5'-GACGTTCAGCGCGAATGATGGTTT (*gmk*) on a CFX96 real-time PCR instrument (BioRad). Relative changes in mRNA levels were determined using the $2^{-\Delta\Delta CT}$ method described previously (Livak & Schmittgen, 2001) by simultaneous normalization against multiple reference genes *rpoA*, *gyrB*, and *gmk* transcript levels (Vandesompele *et al.*, 2002). M values indicated in the figure legends were calculated according to Vandesompele et al. (Vandesompele et al., 2002).

### Fluorescent microscopy

For fluorescent microscopy analysis, cells were grown to mid-log phase and fixed by addition of final 5% formaldehyde. Hooks were stained using monoclonal anti-hemagglutinin coupled to Alexa Fluor488 (Invitrogen). Fixed cells were immobilized using poly-L-lysine treated coverslips. DNA and membrane staining was performed using Hoechst (Invitrogen) and FM-64 (0.5 μg/ml, Invitrogen). Images were collected using an Applied Precision optical sectioning microscope with optical Z sections every 100 nm and deconvolved using softWoRx v.3.4.2 (Applied Precision). The pixel data of individual Z sections of the deconvolved images were projected on a single plane using the Quick Projection tool (settings: maximal intensity) of softWoRx Explorer v1.3 (Applied Precision) and used for quantitative scoring of the number of hook-basal-body complexes per cell.

## Supplementary Material

Refer to Web version on PubMed Central for supplementary material.

## Acknowledgments

This work was supported by PHS grant GM056141 from the National Institutes of Health. We thank Christopher E. Wozniak for helpful comments on how to quantify the number of hook-basal-body complexes and Fabienne F. V. Chevance and Christopher E. Wozniak for strain construction. We also thank Yichi Su and Anoush Emrazian for technical assistance and the Hughes lab for useful discussions of the manuscript. M.E. gratefully acknowledges scholarship support of the Boehringer Ingelheim Fonds.

## References

Aberg A, Fernandez-Vazquez J, Cabrer-Panes JD, Sanchez A, Balsalobre C. Similar and divergent effects of ppGpp and DksA deficiencies on transcription in *Escherichia coli*. J Bacteriol. 2009; 191:3226–3236. [PubMed: 19251846]

Abramoff MD, Magelhaes PJ, Ram SJ. Image Processing with ImageJ. Biophotonics International. 2004; 11:36–42.

Akeda, Galan. Chaperone release and unfolding of substrates in type III secretion. Nature. 2005; 437:911–915. [PubMed: 16208377]

Anderson RP, Roth JR. Tandem genetic duplications in *Salmonella typhimurium*: amplification of the histidine operon. J Mol Biol. 1978; 126:53–71. [PubMed: 368342]

Berg. The rotary motor of bacterial flagella. Annu. Rev. Biochem. 2003; 72:19–54. [PubMed: 12500982]

Berg HC, Anderson RA. Bacteria swim by rotating their flagellar filaments. Nature. 1973; 245:380–382. [PubMed: 4593496]

Chevance FFV, Hughes KT. Coordinating assembly of a bacterial macromolecular machine. Nat Rev Micro. 2008; 6:455–465.

Clegg S, Hughes KT. FimZ is a molecular link between sticking and swimming in *Salmonella enterica* serovar Typhimurium. J Bacteriol. 2002; 184:1209–1213. [PubMed: 11807085]

Ellermeier CD, Slauch JM. RtsA and RtsB coordinately regulate expression of the invasion and flagellar genes in *Salmonella enterica* serovar Typhimurium. J Bacteriol. 2003; 185:5096–5108. [PubMed: 12923082]

Gillen KL, Hughes KT. Molecular characterization of *flgM*, a gene encoding a negative regulator of flagellin synthesis in *Salmonella typhimurium*. J Bacteriol. 1991; 173:6453–6459. [PubMed: 1655712]

Gonzalez-Pedrajo B, Minamino T, Kihara M, Namba K. Interactions between C ring proteins and export apparatus components: a possible mechanism for facilitating type III protein export. Mol Microbiol. 2006; 60:984–998. [PubMed: 16677309]

Hughes, Gillen, Semon, Karlinsey. Sensing structural intermediates in bacterial flagellar assembly by export of a negative regulator. Science. 1993; 262:1277–1280. [PubMed: 8235660]

Kelly A, Goldberg MD, Carroll RK, Danino V, Hinton JC, Dorman CJ. A global role for Fis in the transcriptional control of metabolism and type III secretion in *Salmonella enterica* serovar Typhimurium. Microbiology. 2004; 150:2037–2053. [PubMed: 15256548]

Komeda Y, Suzuki H, Ishidsu JI, Iino T. The role of cAMP in flagellation of *Salmonella typhimurium*. Mol Gen Genet. 1976; 142:289–298. [PubMed: 178991]

Konishi M, Kanbe M, McMurry JL, Aizawa SI. Flagellar formation in C-ring defective mutants by overproduction of FliI, the ATPase specific for the flagellar type III secretion. J Bacteriol. 2009

Kubori T, Shimamoto N, Yamaguchi S, Namba K, Aizawa S. Morphological pathway of flagellar assembly in *Salmonella typhimurium*. J Mol Biol. 1992; 226:433–446. [PubMed: 1640458]

Kugelberg E, Kofoid E, Reams AB, Andersson DI, Roth JR. Multiple pathways of selected gene amplification during adaptive mutation. Proc Natl Acad Sci U S A. 2006; 103:17319–17324. [PubMed: 17082307]

Kutsukake K. Autogenous and global control of the flagellar master operon, *flhD*, in *Salmonella typhimurium*. Mol Gen Genet. 1997; 254:440–448. [PubMed: 9180698]

Lee, Wozniak, Karlinsey, Hughes. Genomic screening for regulatory genes using the T-POP transposon. Meth Enzymol. 2007; 421:159–167. [PubMed: 17352922]

Lee HJ, Hughes KT. Posttranscriptional control of the *Salmonella enterica* flagellar hook protein FlgE. J Bacteriol. 2006; 188:3308–3316. [PubMed: 16621824]

Lehnen D, Blumer C, Polen T, Wackwitz B, Wendisch VF, Unden G. LrhA as a new transcriptional key regulator of flagella, motility and chemotaxis genes in *Escherichia coli*. Mol Microbiol. 2002; 45:521–532. [PubMed: 12123461]

Libby SJ, Goebel W, Ludwig A, Buchmeier N, Bowe F, Fang FC, Guiney DG, Songer JG, Heffron F. A cytolysin encoded by *Salmonella* is required for survival within macrophages. Proc Natl Acad Sci U S A. 1994; 91:489–493. [PubMed: 8290552]

Liu X, Matsumura P. The FlhD/FlhC complex, a transcriptional activator of the *Escherichia coli* flagellar class II operons. J Bacteriol. 1994; 176:7345–7351. [PubMed: 7961507]

Livak KJ, Schmittgen TD. Analysis of relative gene expression data using real-time quantitative PCR and the 2(−ΔΔC(T)) Method. Methods. 2001; 25:402–408. [PubMed: 11846609]

Macnab R. How bacteria assemble flagella. Annu. Rev. Microbiol. 2003; 57:77–100. [PubMed: 12730325]

Majdalani N, Gottesman S. The Rcs phosphorelay: a complex signal transduction system. Annu Rev Microbiol. 2005; 59:379–405. [PubMed: 16153174]

Miller JH. Experiments in Molecular Genetics. Cold Spring Harbor Laboratory, NY. 1972:352–355.

Minamino, Macnab. Components of the *Salmonella* flagellar export apparatus and classification of export substrates. J. Bacteriol. 1999; 181:1388–1394. [PubMed: 10049367]

Minamino T, Namba K. Distinct roles of the FliI ATPase and proton motive force in bacterial flagellar protein export. Nature. 2008; 451:485. [PubMed: 18216858]

Ohnishi K, Kutsukake K, Suzuki H, Iino T. Gene *fliA* encodes an alternative sigma factor specific for flagellar operons in *Salmonella typhimurium*. Mol Gen Genet. 1990; 221:139–147. [PubMed: 2196428]

Paul K, Erhardt M, Hirano T, Blair DF, Hughes KT. Energy source of flagellar type III secretion. Nature. 2008; 451:489–492. [PubMed: 18216859]

Rappleye CA, Roth JR. A Tn*10* derivative (T-POP) for isolation of insertions with conditional (tetracycline-dependent) phenotypes. J Bacteriol. 1997; 179:5827–5834. [PubMed: 9294441]

Saini S, Brown JD, Aldridge PD, Rao CV. FliZ Is a posttranslational activator of FlhD4C2-dependent flagellar gene expression. J Bacteriol. 2008; 190:4979–4988. [PubMed: 18469103]

Sanderson KE, Roth JR. Linkage map of *Salmonella typhimurium*, Edition VI. Microbiol. Rev. 1983; 47:410–453. [PubMed: 6314110]

Simm R, Remminghorst U, Ahmad I, Zakikhany K, Romling U. A role for the EAL-like protein STM1344 in regulation of CsgD expression and motility in *Salmonella enterica* serovar Typhimurium. J Bacteriol. 2009; 191:3928–3937. [PubMed: 19376870]

Soutourina O, Kolb A, Krin E, Laurent-Winter C, Rimsky S, Danchin A, Bertin P. Multiple control of flagellum biosynthesis in *Escherichia coli*: role of H-NS protein and the cyclic AMP-catabolite activator protein complex in transcription of the *flhDC* master operon. J Bacteriol. 1999; 181:7500–7508. [PubMed: 10601207]

Spaeth KE, Chen YS, Valdivia RH. The *Chlamydia* type III secretion system C-ring engages a chaperone-effector protein complex. PLoS Pathog. 2009; 5:e1000579. [PubMed: 19750218]

Spory A, Bosserhoff A, von Rhein C, Goebel W, Ludwig A. Differential regulation of multiple proteins of *Escherichia coli* and *Salmonella enterica* serovar Typhimurium by the transcriptional regulator SlyA. J Bacteriol. 2002; 184:3549–3559. [PubMed: 12057949]

Stojiljkovic I, Baumler AJ, Hantke K. Fur regulon in gram-negative bacteria. Identification and characterization of new iron-regulated *Escherichia coli* genes by a fur titration assay. J Mol Biol. 1994; 236:531–545. [PubMed: 8107138]

Takaya A, Matsui M, Tomoyasu T, Kaya M, Yamamoto T. The DnaK chaperone machinery converts the native $FlhD_2C_2$ hetero-tetramer into a functional transcriptional regulator of flagellar regulon expression in *Salmonella*. Mol Microbiol. 2006; 59:1327–1340. [PubMed: 16430704]

Tomoyasu T, Takaya A, Isogai E, Yamamoto T. Turnover of FlhD and FlhC, master regulator proteins for *Salmonella* flagellum biogenesis, by the ATP-dependent ClpXP protease. Mol Microbiol. 2003; 48:443–452. [PubMed: 12675803]

Vandesompele J, De Preter K, Pattyn F, Poppe B, Van Roy N, De Paepe A, Speleman F. Accurate normalization of real-time quantitative RT-PCR data by geometric averaging of multiple internal control genes. Genome Biol. 2002; 3 RESEARCH0034.

Wang Q, Zhao Y, McClelland M, Harshey RM. The RcsCDB signaling system and swarming motility in *Salmonella enterica* serovar typhimurium: dual regulation of flagellar and SPI-2 virulence genes. J Bacteriol. 2007; 189:8447–8457. [PubMed: 17905992]

Wang S, Fleming RT, Westbrook EM, Matsumura P, McKay DB. Structure of the *Escherichia coli* FlhDC complex, a prokaryotic heteromeric regulator of transcription. J Mol Biol. 2006; 355:798–808. [PubMed: 16337229]

Wei BL, Brun-Zinkernagel AM, Simecka JW, Pruss BM, Babitzke P, Romeo T. Positive regulation of motility and *flhDC* expression by the RNA-binding protein CsrA of *Escherichia coli*. Mol Microbiol. 2001; 40:245–256. [PubMed: 11298291]

Wozniak CE, Lee C, Hughes KT. T-POP array identifies EcnR and PefI-SrgD as novel regulators of flagellar gene expression. Journal of Bacteriology. 2008

Yamamoto S, Kutsukake K. FliT acts as an anti-$FlhD_2C_2$ factor in the transcriptional control of the flagellar regulon in *Salmonella enterica* serovar typhimurium. J Bacteriol. 2006; 188:6703–6708. [PubMed: 16952964]

Yanagihara S, Iyoda S, Ohnishi K, Iino T, Kutsukake K. Structure and transcriptional control of the flagellar master operon of *Salmonella typhimurium*. Genes Genet Syst. 1999; 74:105–111. [PubMed: 10586519]

Zhang X, Bremer H. Control of the *Escherichia coli rrnB* P1 promoter strength by ppGpp. J Biol Chem. 1995; 270:11181–11189. [PubMed: 7538113]

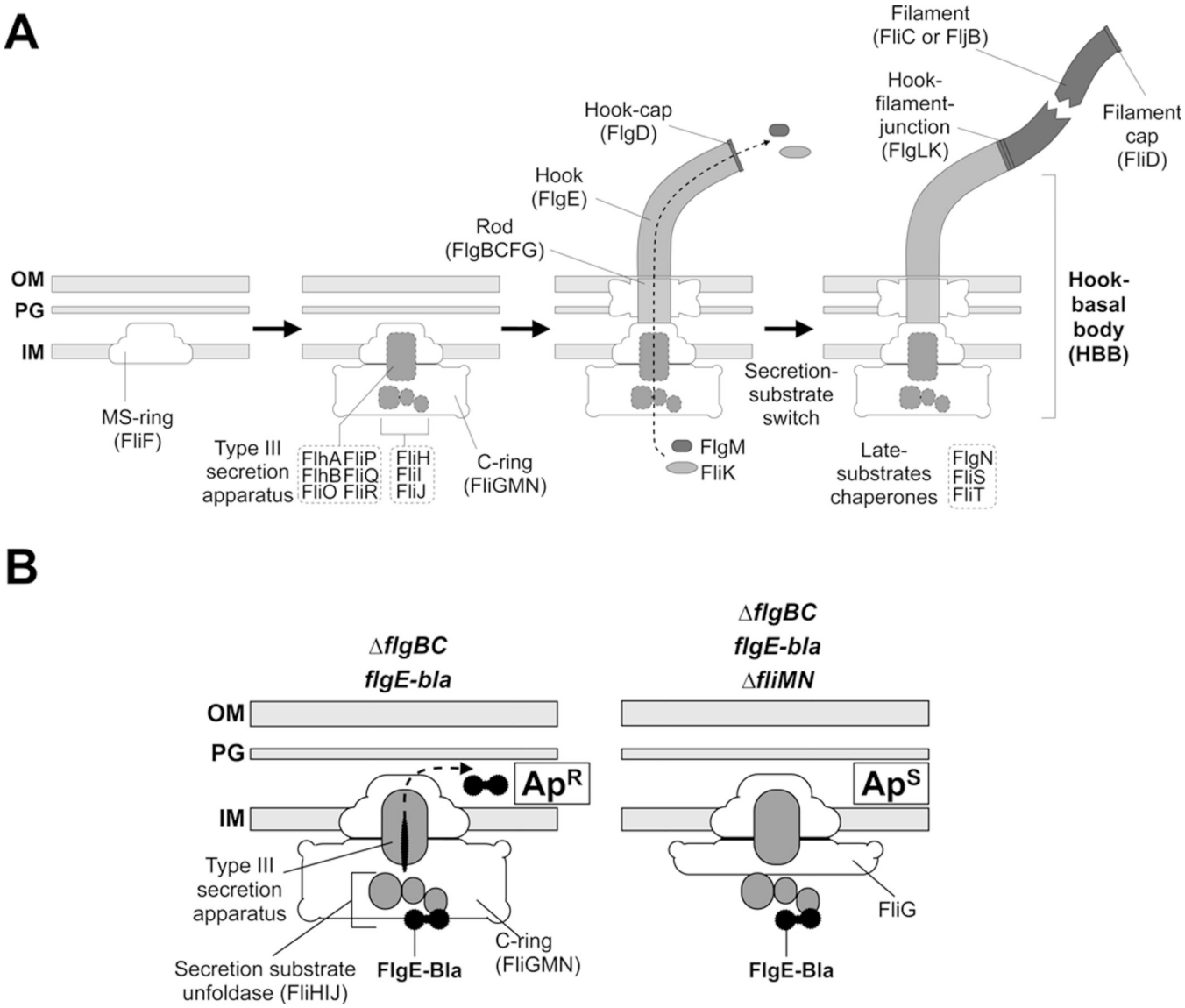


**Figure 1.**

**(A) Steps in the assembly of the bacterial flagellum.** The self-assembly process of the flagellum initiates with formation of the MS-ring (FliF) in the cytoplasmic membrane. Afterwards, a flagellar-specific type III secretion (T3S) apparatus assembles within a central pore of the MS-ring and the C-ring is attached to the cytoplasmic face of the MS-ring. At this point, flagellar secretion substrates are now selectively secreted via the T3S apparatus and coupled to the proton-motive force (Paul et al., 2008). The hook polymerizes to an app. length of 55 nm that is determined by the molecular ruler FliK and this triggers a secretion specificity switch from rod-hook-type substrates to late-secretion substrates. Upon completion of the hook-basal-body complex, the negative regulator of late substrates gene expression, the anti-$\sigma^{28}$ factor FlgM, is secreted thereby freeing $\sigma^{28}$ to initiate transcription of late substrate genes, like *fliC* or the genes of the chemosensory system.

**(B) Hook-β-lactamase reporter system.** Left panel: In a strain deleted for the proximal rod subunit genes, *flgBC*, hook-basal-body type substrates are secreted via the flagellar-specific T3S apparatus into the periplasm and subsequently degraded. β-lactamase (Bla) fused C-terminally to the hook protein FlgE is not degraded and confers resistance against lactam

antibiotics, like ampicillin when secreted into the periplasm ($Ap^R$). Right panel: In a strain additionally deleted for two-thirds of the cytoplasmic C-ring (Δ*fliMN*), flagellar T3S is severely impaired and thus FlgE-Bla is not secreted into the periplasm and the strain is sensitive against ampicillin ($Ap^S$).

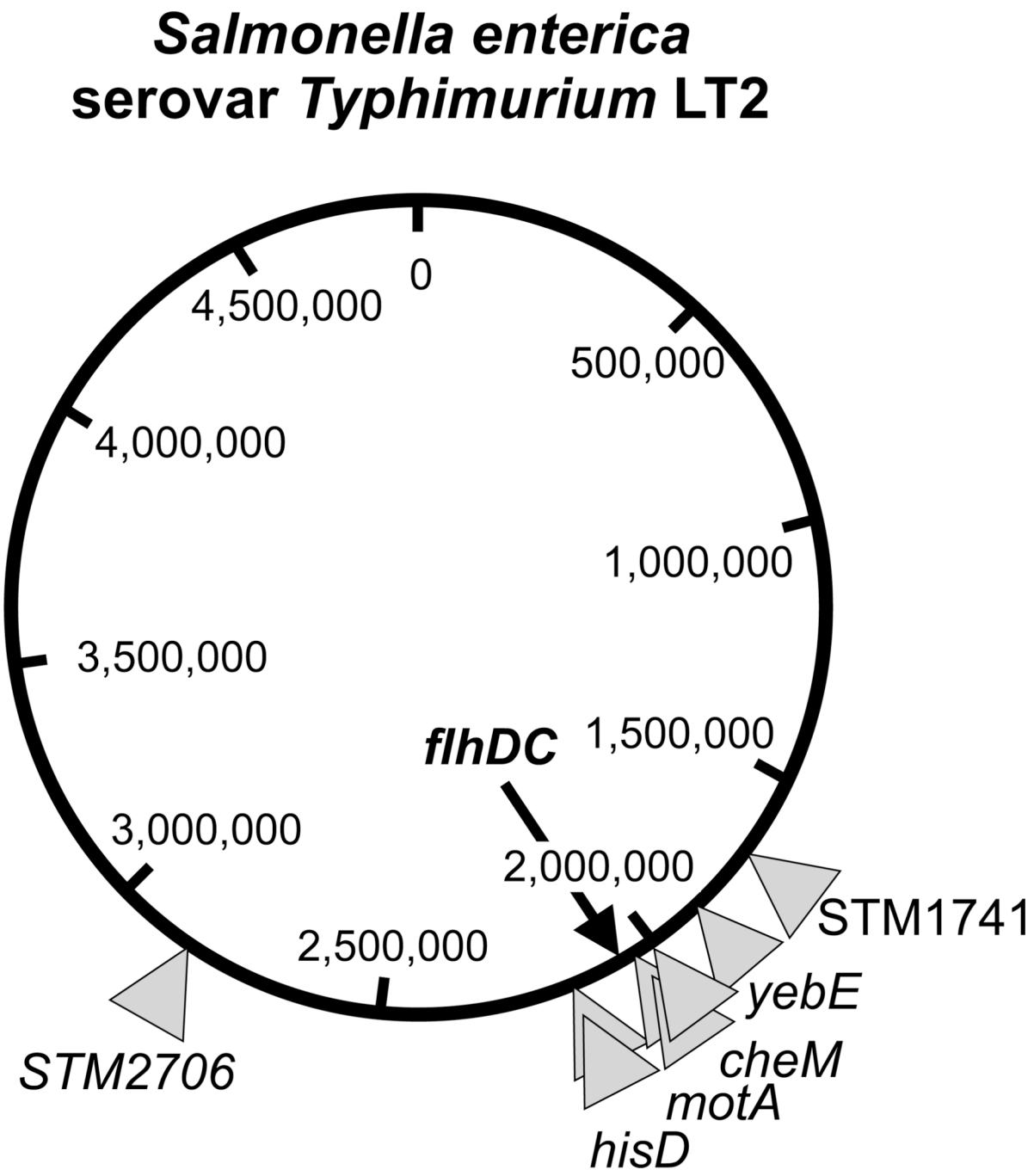


**Figure 2. Locations of unstable Mu*d* insertions in the *Salmonella* chromosome in strains duplicated for the *flhDC* region that conferred ampicillin resistance in the absence of the C-ring**

The positions of eight $Ap^R$ Mu*d* insertions in the *Salmonella* chromosome were determined by DNA sequence analysis. Individual Mu*d* insertions are indicated by a grey triangle and additionally the chromosomal loci of the insertions. These unstable $Ap^R$ Mu*d* insertions resulted from transposition into duplications of the *flhDC* region of the chromosome thus conferring ampicillin resistance in the absence of the C-ring by increased *flhDC* expression. The precise insertion points are given in Table 1.

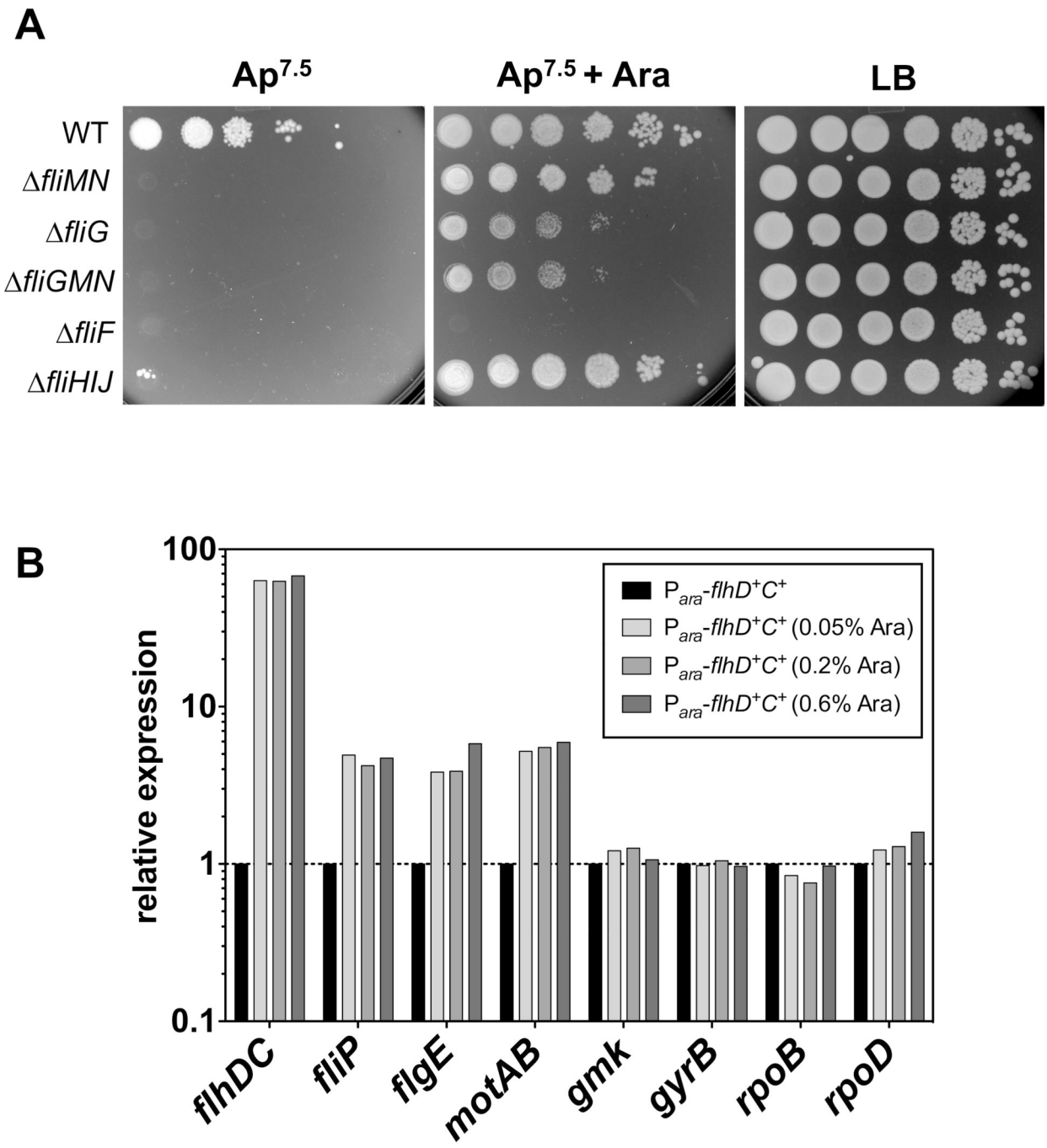


**Figure 3.**

**(A) Overexpression of *flhDC* from the arabinose promoter confers ampicillin resistance in deletion mutants of the C-ring and ATPase complex.** Strains harboring an additional, functional copy of *flhDC* under the control of the arabinose promoter were grown overnight in the absence of arabinose. Equal volumes of ten-fold serial dilutions were spotted on LB plates and PPBS $Ap^{7.5}$ plates in the presence or absence of 0.2 % arabinose. Mutant strains missing two-thirds (Δ*fliMN*) or the complete C-ring (Δ*fliG* and Δ*fliGMN*), as well as a strain deleted for the ATPase complex FliHIJ, but not a mutant strain missing the MS-ring (Δ*fliF*) are able grow in the presence of excess FlhDC. WT = TH14902; Δ*fliMN* = TH15498; Δ*fliG* = TH15497; Δ*fliGMN* = TH14906; Δ*fliF* = TH14903; Δ*fliHIJ* = TH14905.

**(B) Effects of excess FlhDC on flagellar gene expression.** Strain TH14156 ($P_{ara}$::*flhD*$^{+}$*C*$^{+}$) was grown for 2.5 hours in LB media containing different concentrations of arabinose (0%, 0.05%, 0.2% and 0.6%) and total RNA was isolated of the pooled cultures of three biological replicates. Class 1 (*flhDC*), Class 2 (*fliP* and flgE), Class 3 (*motAB*) and *rpoD* transcript levels were analyzed by real-time qPCR as described in Experimental procedures. Relative gene expression was determined using the $2^{-\Delta\Delta CT}$ method (Livak & Schmittgen, 2001) and individual mRNA levels were normalized against multiple reference genes (*rpoB, gyrB* and *gmk*) and presented as fold change relative against the wildtype control (Vandesompele et al., 2002).

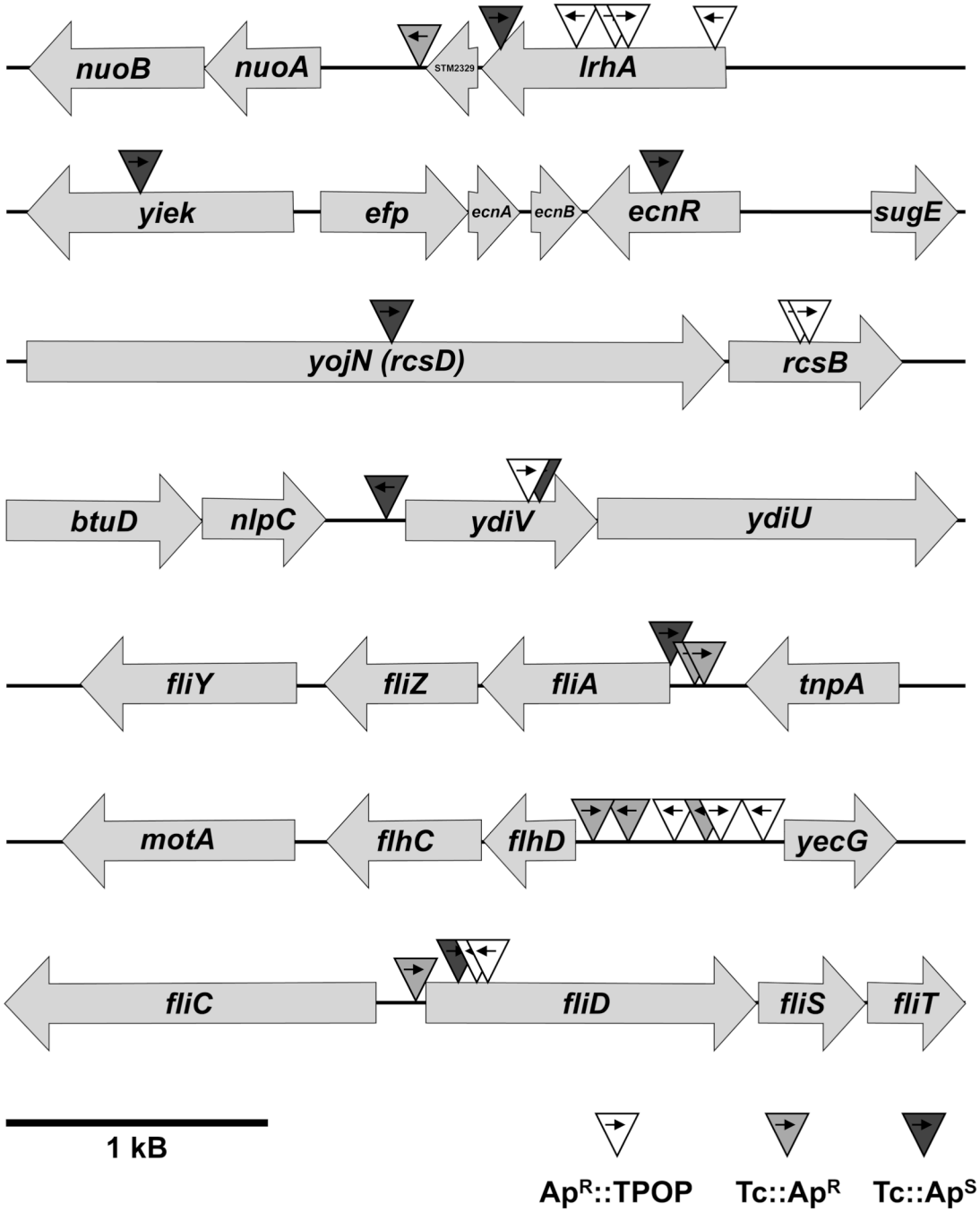


**Figure 4. Schematic overview of T-POP insertions at seven different chromosomal loci that conferred ampicillin resistance in a C-ring deletion mutant**

Individual T-POP insertions are shown by a triangle with an arrow indicating the direction of the *tetA* transcript. A summary of the precise insertion point of every T-POP insertion and the effect of the *tetA* transcript reading in adjacent chromosomal genes is given in Table 2.

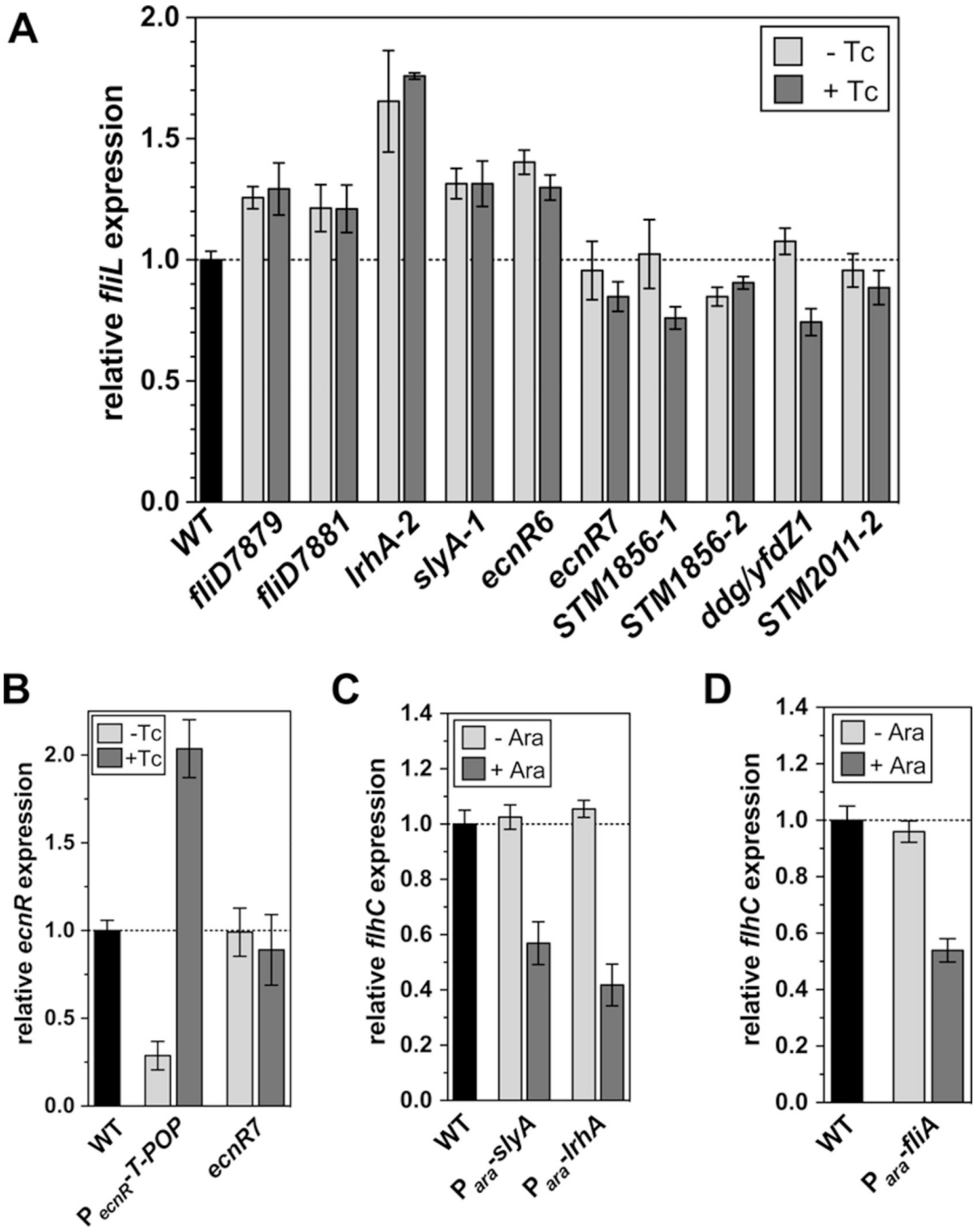


**Figure 5.**

**(A) Relative flagellar Class 2 transcription levels of selected, ampicillin-resistance conferring, T-POP insertions.** Relative Class 2 transcription from the *fliL*::Mu*dJ* transcriptional reporter was measured by β-galactosidase assays as described in Experimental procedures. Class 2 transcription was measured in the presence or absence of tetracycline and normalized against the wildtype control. Addition of tetracycline induces transcription from the *tetA* promoter, which proceeds into chromosomal DNA adjacent to the T-POP insertion. The data shown are the mean +/− SD of at least three independent, biological replicates.

**(B) Relative *ecnR* transcription in a strain with a T-POP insertion in *yiek* near *ecnR*.** Relative *ecnR* transcription from the *ecnR*::Mu*dJ* transcriptional reporter was measured by β-galactosidase assays as described in Experimental procedures in strains harboring a T-POP insertion upstream of *ecnR* ($P_{ecnR}$::T-POP) or in *yiek* near *ecnR* (*ecnR7*). *ecnR* transcription was measured in the presence or absence of tetracycline and normalized against the wildtype control. The data shown are the mean +/− SD of at least three independent, biological replicates.

**(C) Relative flagellar Class 1 transcription in strains overexpressing the transcriptional regulators SlyA and LrhA.** Relative Class 1 transcription from the *flhC*::Mu*dJ* transcriptional reporter was measured by β-galactosidase assays as described in Experimental procedures in strains harboring *slyA* or *lrhA* under control of the arabinose promoter. Class 1 transcription was measured in the presence or absence of 0.2 % arabinose, respectively and normalized against the wildtype control. The data shown are the mean +/− SD of at least three independent, biological replicates.

**(D) Relative flagellar Class 1 transcription in a strain overexpressing the flagellar-specific sigma factor $\sigma^{28}$.** Relative Class 1 transcription from the *flhC*::Mu*dJ* transcriptional reporter was measured by β-galactosidase assays as described in Experimental procedures in a strain harboring *fliA*, the gene encoding for the flagellar-specific sigma factor $\sigma^{28}$, under control of the arabinose promoter. Class 1 transcription was measured in the presence or absence of 0.2 % arabinose, respectively and normalized against the wildtype control. The data shown are the mean +/− SD of at least three independent, biological replicates.

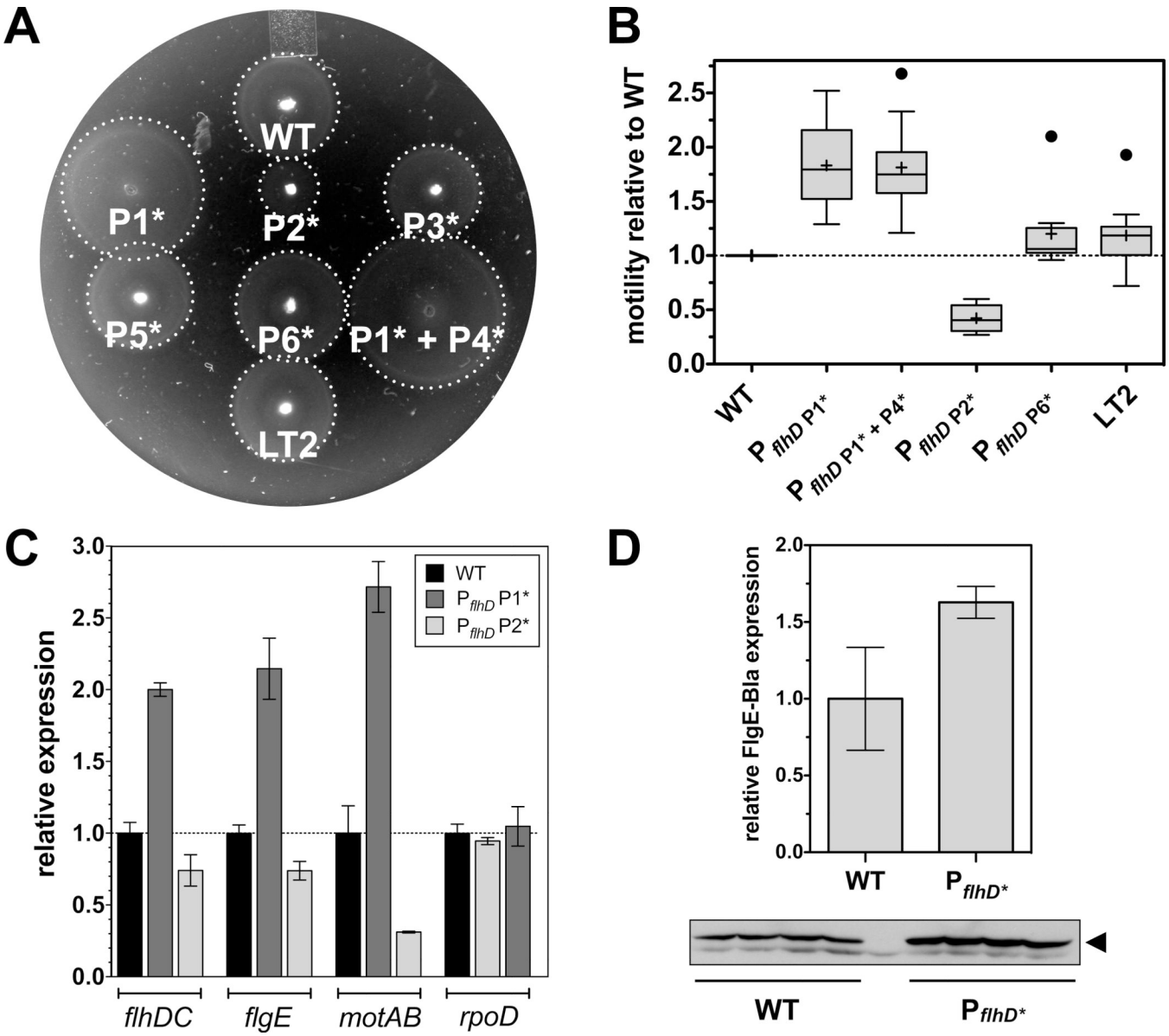


**Figure 6. Motility, flagellar Class 1 and Class transcription and FlgE-Bla protein levels of $P_{flhD}$ promoter mutants**

**(A) Motility of $P_{flhD}$ promoter mutants.** A representative image shows the motility of different $P_{flhD}$ promoter mutants after 4 hours of incubation at 37°C. A dotted white line indicates the radius of the swarming circle. Consensus -10 box mutants of the P3, P5 and P6 *flhD* promoter display motility comparable to wildtype. The consensus -10 box mutant of the P1 *flhD* promoter and the combination of the consensus -10 box mutations of both the P1 and P4 *flhD* promoter showed increased swimming behavior, whereas the consensus -10 box mutation of the P2 *flhD* promoter displayed a decreased swimming speed. The $P_{flhD}$ promoter mutants were constructed in a strain harboring a functional *fliM-gfp* mutation (denoted here as WT). Motility was compared to *S. enterica* LT2 to show that the *fliM-gfp* mutation did not affect flagellar assembly or motility.

**(B) Quantitative motility assay of $P_{flhD}$ promoter mutants.** The motility of different mutant strains was measured by determining the motility diameter after 4 hours incubation at 37 °C. For each strain the diameter of 10 independent biological replicates was measured

and normalized to the motility diameter of the wildtype control (*fliM-gfp*) on the same motility plate. Motility was compared to *S. enterica* LT2 to show that the *fliM-gfp* mutation did not affect flagellar assembly or motility. The data is presented as box diagrams with whiskers according to the Tukey method. A horizontal line indicates the median and a black cross the mean. Outliners are represented by a black dot.

**(C) Relative Class 1, Class 2 and Class 3 mRNA levels as quantified by real-time qPCR.** Class 1 (*flhDC*), Class 2 (*flgE*), Class 3 (*motAB*) and *rpoD* mRNA levels were analyzed by real-time qPCR as described in Experimental procedures. Relative gene expression was determined using the $2^{-\Delta\Delta CT}$ method (Livak & Schmittgen, 2001). Individual mRNA levels were normalized against *rpoA*, *gyrB* and *gmk* transcript levels and presented as fold change relative against the wildtype control (Vandesompele et al., 2002). The data shown represents the mean of three independent, biological samples ± SD.

**(D) Relative FlgE-Bla protein levels analyzed by quantitative Western blotting.** Whole cell lysates were prepared of four independent biological replicates of wildtype or P1 + P4 consensus -10 box *flhD* promoter mutant cells respectively. The experiment was performed in a Δ*fliP* background in order to analyze total protein levels. The reporter protein FlgE-Bla was expressed from its native promoter and FlgE-Bla was detected using FlgE-specific antibodies and quantified as described in Experimental procedures. Data shown are the mean of four replicates ± SD.

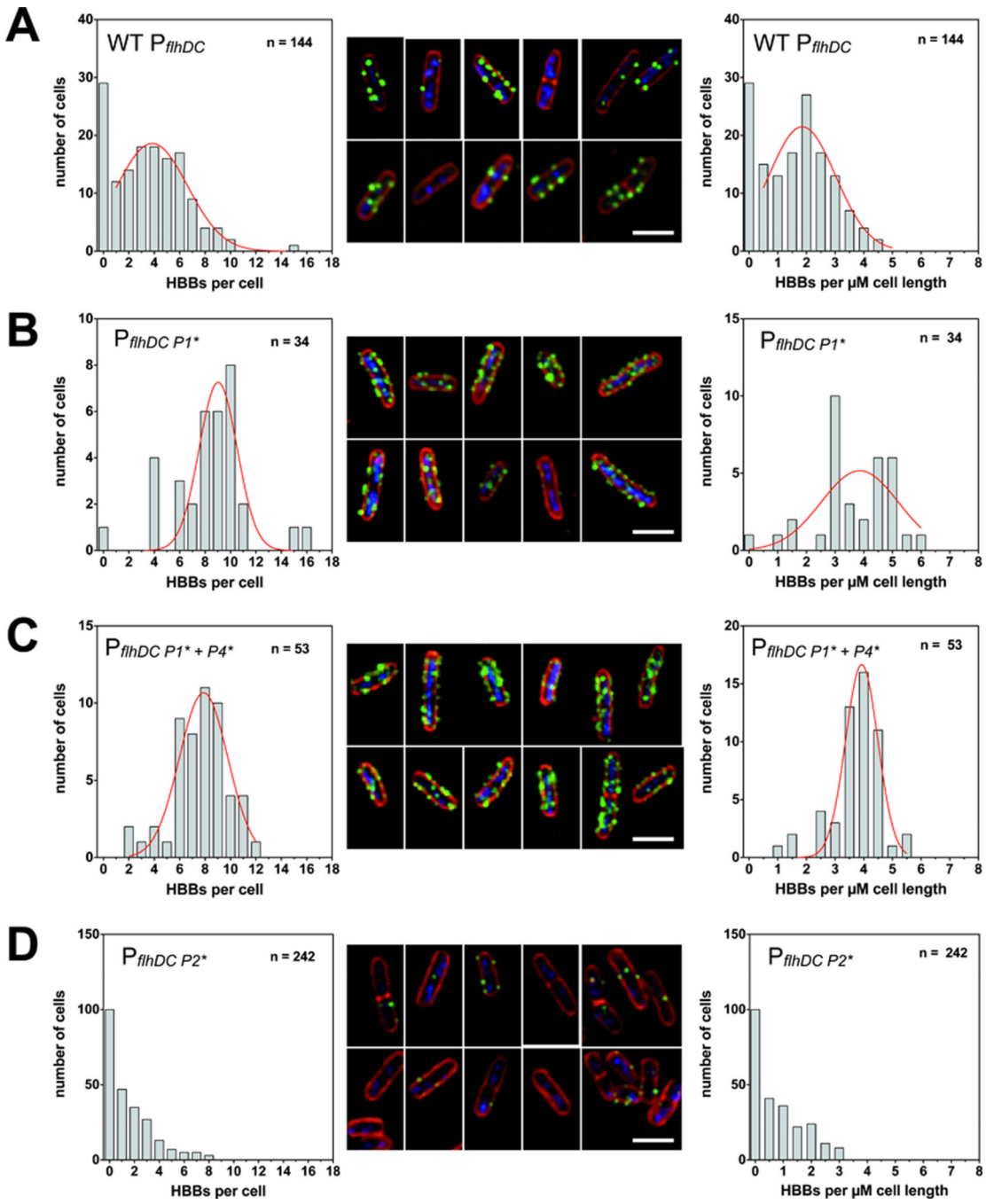


**Figure 7. Number of assembled hook-basal-body (HBB) complexes as analyzed by hook immunostaining**

**(A) Number of HBB complexes of the wildtype control.** Left panel: distribution of HBBs per cell. Non-linear fitting of the Gaussian distribution was employed (red line) and the average HBB number per cell is 3.8 ± 2.8 (n = 144). Middle panel: hook immunostaining of exemplary cells expressing wildtype levels of *flhDC*. Green: HBB complexes (FlgE::3×HA tag) labeled with anti-hemagglutinin antibodies coupled to Alexa Fluor 488. Red: cell membrane stained with FM-64. Blue: DNA stained with Hoechst. Right panel: distribution of HBBs per µM cell length. Cell length was measured based on the FM-64 membrane

staining. Non-linear fitting of the Gaussian distribution was employed (red line) and the average HBB number per μM is 1.9 ± 1.2 (n = 144). Scale bar is 2 μM.

**(B) Number of HBB complexes of the $P_{flhD}$ P1 consensus -10 box mutant.** Left panel: distribution of HBBs per cell. Non-linear fitting of the Gaussian distribution was employed (red line) and the average HBB number per cell is 9.0 ± 1.5 (n = 34). Middle panel: hook immunostaining of exemplary $P_{flhD}$ P1 consensus -10 box mutant cells with increased *flhDC* expression levels. Green: HBB complexes (FlgE::3×HA tag) labeled with anti-hemagglutinin antibodies coupled to Alexa Fluor 488. Red: cell membrane stained with FM-64. Blue: DNA stained with Hoechst. Right panel: distribution of HBBs per μM cell length. Cell length was measured based on the FM-64 membrane staining. Non-linear fitting of the Gaussian distribution was employed (red line) and the average HBB number per μM is 3.9 ± 1.4 (n = 34). Scale bar is 2 μM.

**(C) Number of HBB complexes of the $P_{flhD}$ P1 + P4 consensus -10 box mutant.** Left panel: distribution of HBBs per cell. Non-linear fitting of the Gaussian distribution was employed (red line) and the average HBB number per cell is 7.9 ± 1.9 (n = 53). Middle panel: hook immunostaining of exemplary $P_{flhD}$ P1 + P4 cinsensus -10 box mutant cells with increased *flhDC* expression levels. Green: HBB complexes (FlgE::3×HA tag) labeled with anti-hemagglutinin antibodies coupled to Alexa Fluor 488. Red: cell membrane stained with FM-64. Blue: DNA stained with Hoechst. Right panel: distribution of HBBs per μM cell length. Cell length was measured based on the FM-64 membrane staining. Non-linear fitting of the Gaussian distribution was employed (red line) and the average HBB number per μM is 3.9 ± 0.6 (n = 53). Scale bar is 2 μM.

**(D) Number of HBB complexes of the $P_{flhD}$ P2 consensus -10 box mutant.** Left panel: distribution of HBBs per cell. Middle panel: hook immunostaining of exemplary $P_{flhD}$ P2 consensus -10 box mutant cells with decreased *flhDC* expression levels. Green: HBB complexes (FlgE::3×HA tag) labeled with anti-hemagglutinin antibodies coupled to Alexa Fluor 488. Red: cell membrane stained with FM-64. Blue: DNA stained with Hoechst. Right panel: distribution of HBBs per μM cell length. Cell length was measured based on the FM-64 membrane staining. Scale bar is 2 μM.

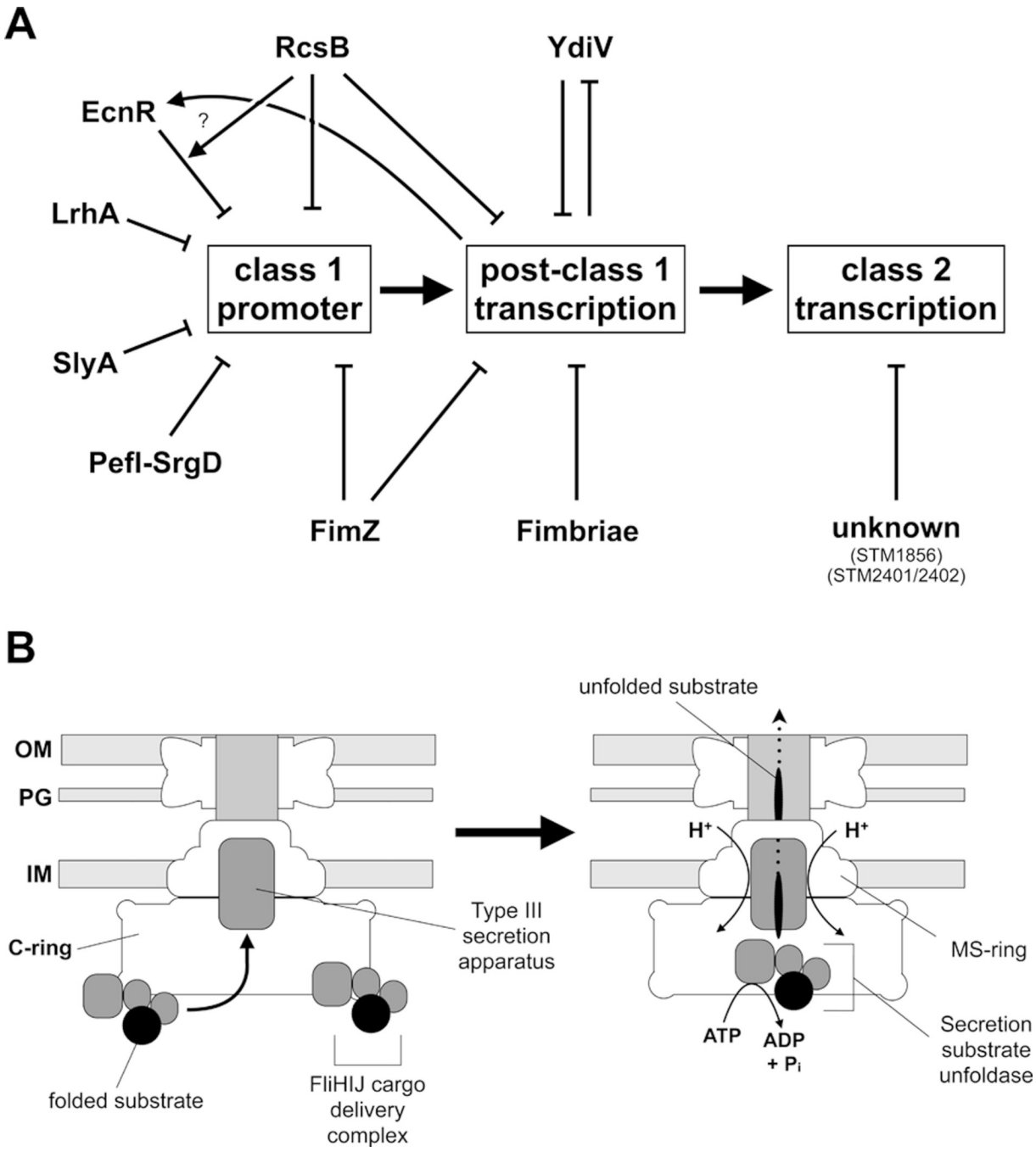


**Figure 8. Regulatory network of flagellar Class 1 gene expression and model for flagellar type III secretion**

**(A) Schematic representation of the regulatory network of flagellar Class 1 gene expression of *Salmonella enterica*.** Arrows represent interactions between different regulators of flagellar Class 1 transcription or post-class 1 transcription. LrhA (Lehnen et al., 2002) and SlyA (Spory et al., 2002) have been previously identified as regulators of *flhDC* and FliC respectively in *Escherichia coli*. Our T-POP mutagenesis identified LrhA and SlyA as negative regulators of *flhDC* expression in *Salmonella enterica*, as well as several known regulators like EcnR (Wozniak et al., 2008) or RcsB (Wang et al., 2007). We also identified several putative regulators of Class 2 transcription like STM1856 and STM2401/STM2402.

**(B) Model of the role of the C-ring affinity cup in flagellar type III secretion.** Folded secretion substrates in complex with the cargo delivery complex FliHIJ dock to affinity sites of the C-ring awaiting secretion. Before PMF-dependent secretion, the secretion substrates are presumably unfolded using ATP-hydrolysis of the ATPase FliI thereby increasing the efficiency of the secretion process. The C-ring presumably acts as an affinity cup to enhance the specificity and efficiency of the flagellar type III secretion process under wildtype conditions by recruiting secretion substrates bound to the FliHIJ cargo delivery complex. Flagellar type III secretion is possible in the absence of the C-ring and ATPase complex if $FlhD_4C_2$ levels are increased. Increased $FlhD_4C_2$ levels result in elevated level of Class 2 secretion substrates and additionally in more potential secretion systems by doubling the number of available basal bodies. Accordingly, increased substrate levels and more potential secretion systems overcome the requirement for both the C-ring and the ATPase complex in flagellar T3S.

## Table 1

**Mu*d* insertions and spontaneous mutations resulting in FlgE-Bla secretion in the absence of the C-ring**

Summary of isolated Mu*d* insertions that transposed into duplicated *flhDC* regions of the chromosome and conferred ampicillin resistance in the C-ring deletion resulting from increased *flhDC* expression. Additionally shown are spontaneous mutations isolated in *fliA* and *flhD* promoter region that also allowed for FlgE-Bla secretion in the absence of the C-ring.

| **Mu*d* insertion** | **location of insertion** |
|---|---|
| *mud2* | 161 bp downstream of *yebE* stop, 39 bp upstream of *ptrB* start |
| *mud4* | 204 bp downstream of *hisD* start |
| *mud10* | 204 bp downstream of hisD start |
| *mud13* | 439 bp downstream of STM2706 start |
| *mud19* | 1308 bp downstream of *cheM* start |
| *mud26* | 1323 bp downstream of *cheM* start |
| *mud32* | 404 bp downstream of STM1741 start |
| *mud36* | 703 bp downstream of *motA* start |
| **allele** | **location of spontaneous mutation** |
| *fliA7463* | *Q106:*STOP (TH14683) |
| *fliA7464* | *Q106:*STOP (TH14684) |
| $P_{flhD}$*7460* | *−38G:A* from *AUG* (TH14680) |
| $P_{flhD}$*7461* | *−152C:T* from *AUG* (TH14681) |

## Table 2

### T-POP transposon insertions that allow for FlgE-Bla secretion in the absence of the C-ring

Summary of isolated T-POP transposon insertions in the C-ring deletion strain TH12470. The *tetA* gene of the T-POP transposon lacks a terminator sequence and therefore genes upstream of *tetA* can be induced by *tetA* expression. If the addition of tetracycline conferred ampicillin resistance, the Tc effect is indicated as Tc-$Ap^R$ and if the addition of tetracycline resulted in an ampicillin sensitive phenotype, the Tc effect is indicated as Tc-$Ap^S$. In all other cases, the T-POP insertion conferred ampicillin resistance on its own and the addition of tetracycline showed no effect ($Ap^R$::TPOP).

| allele | insertion | Tc effect |
|---|---|---|
| *lrhA1* | *lrhA* coding region, 9 bp downstream of ATG | $Ap^R$::TPOP |
| *lrhA2* | *lrhA* coding region, 607 bp downstream of ATG | $Ap^R$::TPOP |
| *lrhA3* | *lrhA* coding region, 536 bp downstream of ATG | $Ap^R$::TPOP |
| *lrhA4* | *lrhA* coding region, 936 bp downstream of ATG | Tc-$Ap^S$ |
| *lrhA5* | STM2329 terminator, 9 bp downstream of stop | Tc-$Ap^R$ |
| *ecnR6* | *ecnR* coding region, 157 bp downstream of ATG | Tc-$Ap^S$ |
| *ecnR7* | *yjek* coding region, 859 bp downstream of ATG | Tc-$Ap^S$ |
| *slyA1* | *slyA* coding region, 170 bp downstream of ATG | $Ap^R$::TPOP |
| *rcsB131* | *rcsB* coding region, 332 bp downstream of ATG | $Ap^R$::TPOP |
| *rcsB132* | *rcsB* coding region, 332 bp downstream of ATG | $Ap^R$::TPOP |
| *yojN253* | *yojN* coding region, 1211 bp downstream of ATG | Tc-$Ap^S$ |
| *ydiV254* | *ydiV* coding region, 634 bp downstream of ATG | $Ap^R$::TPOP |
| *ydiV255* | *ydiV* coding region, 640 bp downstream of ATG | Tc-$Ap^S$ |
| *ydiV256* | *ydiV* promoter, 68 bp upstream of ATG | Tc-$Ap^S$ |
| *clpP71* | *clpP* coding region, 579 bp downstream of ATG | Tc-$Ap^S$ |
| *fliA7876* | *fliA* promoter, 30 bp upstream of ATG | Tc-$Ap^R$ |
| *fliA7877* | *fliA* promoter, 11 bp upstream of ATG | Tc-$Ap^R$ |
| *fliA7878* | *fliA* promoter, 1 bp upstream of ATG | Tc-$Ap^S$ |
| *flhDC7872* | *flhD* promoter, 426 bp upstream of ATG | $Ap^R$::TPOP |
| *flhDC7873* | *flhD* promoter, 625 bp upstream of ATG | $Ap^R$::TPOP |
| *flhDC7874* | *flhD* promoter, 799 bp upstream of ATG | $Ap^R$::TPOP |
| *flhDC7875* | *flhD* promoter, 615 bp upstream of ATG | Tc-$Ap^R$ |
| *flhDC5* | *flhD* promoter, 178 bp upstream of ATG | Tc-Ap$R^R$ |
| *flhDC6* | *flhD* promoter, 22 bp upstream of ATG | Tc-$Ap^R$ |
| *flgM1* | *flgM* coding region, 152 bp downstream of ATG | $Ap^R$::TPOP |
| *flgM2* | *flgA* promoter, 85 bp upstream of ATG | $Ap^R$::TPOP |
| *fliD7879* | *fliD* coding region, 93 bp downstream of ATG | $Ap^R$::TPOP |
| *fliD7880* | *fliD* coding region, 95 bp downstream of ATG | $Ap^R$::TPOP |
| *fliD7881* | *fliD* promoter, 30 bp upstream of ATG | Tc-$Ap^R$ |

| allele | insertion | Tc effect |
|---|---|---|
| *fliD7882* | *fliD* coding region, 85 bp downstream of ATG | Tc-Ap$^S$ |
| *fliR1* | *fliR* coding region, 608 bp downstream of ATG | Ap$^R$::TPOP |
| *STM1856-1* | STM1854 coding region, 5 bp downstream of ATG | Ap$^R$::TPOP |
| *STM1856-2* | STM1856 promoter, 465 bp upstream of ATG | Tc-Ap$^S$ |
| *STM2011-1* | *amn* coding region, 5 bp downstream of ATG | Tc-Ap$^R$ |
| *STM2011-2* | STM2011 promoter, 272 bp upstream of ATG | Tc-Ap$^R$ |
| *rfbP1* | *rfbP* coding region, 1300 bp downstream of ATG | Tc-Ap$^S$ |
| *pgtE1* | *pgtE* coding region, 444 bp downstream of ATG | Tc-Ap$^R$ |
| *ddg/yfdZ1* | *ddg/yfdZ* terminator, 8 bp downstream of ddg stop | Ap$^R$::TPOP |
| *pykF1* | *pykF* terminator, 264 bp downstream of pykF stop | Tc-Ap$^R$ |
| *garL1* | *garL* coding region, 74 bp downstream of ATG | Ap$^R$::TPOP |
| *yieP1* | *yieP* coding region, 398 bp downstream of ATG | Tc-Ap$^R$ |
| *hpaX1* | *hpaX* coding region, 196 bp downstream of ATG | Tc-Ap$^R$ |